Accepted Manuscript

Title: The kinematic history of the Khlong Marui and Ranong Faults, Southern Thailand

Authors: Ian Watkinson, Chris Elders, Robert Hall

PII: S0191-8141(08)00148-X
DOI: 10.1016/j.jsg.2008.09.001
Reference: SG 2186

To appear in: *Journal of Structural Geology*

Received Date: 19 February 2008
Revised Date: 1 September 2008
Accepted Date: 9 September 2008

Please cite this article as: Watkinson, I., Elders, C., Hall, R. The kinematic history of the Khlong Marui and Ranong Faults, Southern Thailand, Journal of Structural Geology (2008), doi: 10.1016/j.jsg.2008.09.001

The kinematic history of the Khlong Marui and Ranong Faults, Southern Thailand

Ian Watkinson*, Chris Elders, Robert Hall

SE Asia Research Group, Department of Geology, Royal Holloway, University of London, Egham, Surrey, TW20 0EX, United Kingdom

Abstract

The Khlong Marui Fault (KMF) and Ranong Fault (RF) are major NNE trending strike-slip faults which dissect peninsular Thailand. They have been assumed to be conjugate to the NW-trending Three Pagodas Fault (TPF) and Mae Ping Fault (MPF) in Northern Thailand, which experienced a diachronous reversal in shear sense during India – Eurasia collision. It follows that the KMF and RF are expected to show the opposite shear sense and an inversion at a similar time to the TPF and MPF. New field data from the KMF and RF reveal two phases of ductile dextral shear separated by Campanian magmatism. Paleocene to Eocene post-kinematic granites date the end of this phase, while a brittle sinistral phase deforms the granites, and has exhumed the metamorphic rocks. The timing of these movements precludes formation of the faults in response to Himalayan extrusion tectonics. Instead, they formed near the southern margin of a late Cretaceous – Paleocene orogen, and may have been

* *Corresponding author. SE Asia Research Group, Department of Geology, Royal Holloway, University of London, Egham, Surrey, TW20 0EX, United Kingdom. Tel: +441784 443611; fax: +441784 434716.*

E-mail address: i.watkinson@gl.rhul.ac.uk (Ian Watkinson).

influenced by variations in the rate of subduction ahead of India and Australia. North-south compression prior to reactivation of the subduction zone around southern Sundaland in the Eocene caused widespread deformation in the over-riding plate, including sinistral transpression on the KMF and RF.

Keywords

Strike-slip faults; Fault kinematics; Lateral extrusion; Ductile shear zone; Thailand; Sundaland

1.0 Introduction

Widespread intraplate deformation within mainland Southeast Asia is conspicuously expressed by northwest trending strike-slip faults which originate near the eastern Himalayan syntaxis. These include the Ailao Shan – Red River Fault (ASRR), the Mae Ping Fault (MPF), and the Three Pagodas Fault (TPF) (Fig. 1), which are interpreted to have played a key role in the eastwards movement of fault-bounded blocks during indentation of the Indian continent into the Eurasian plate (e.g. Gilley et al., 2003; Lacassin et al., 1997; Leloup et al., 1995; Tapponnier et al., 1982, 1986). They record a history of sinistral motion under medium to high metamorphic conditions followed by a diachronous reversal in shear sense and a change to brittle deformation during the Oligocene on the TPF and MPF, and the Miocene on the ASRR (Gilley et al., 2003; Lacassin et al., 1997; Leloup et al., 1995, 2001; Wang et al., 1998). Northward-younging slip sense reversal is believed to result from northward

migration of the Himalayan deformation front and lateral extrusion of successive fault-bounded blocks (Lacassin et al., 1997).

The northeast-trending Khlong Marui Fault (KMF) and Ranong Fault (RF) (Fig. 2) cut across the Thai Peninsula south of the NW trending faults, and are orientated about 100° anti-clockwise of the TPF (Fig. 1). Although they have not been traced offshore, the two fault zones appear to intersect in the northern Gulf of Thailand. As a result, the KMF and RF have been interpreted to be conjugate to the TPF and MPF (Lacassin et al., 1997; Tapponnier et al., 1986), an assumption which has become entrenched in subsequent references to the Tertiary deformation of the area. Their kinematics are therefore modeled as ductile dextral motion during the early stages of India – Eurasia collision, changing to brittle sinistral at the same time as the change from sinistral to dextral on the TPF and MPF (e.g. Hall, 1996, 2002; Lee and Lawver, 1995; Replumaz and Tapponnier, 2003; Tapponnier et al., 1986).

Development of the South China Sea, and Tertiary basins of offshore Vietnam, Cambodia and in Northern Thailand, have also been attributed to movement on the NW-trending strike-slip faults (Briais et al., 1993, Polachan et al., 1991; Tapponnier et al., 1986), and offshore extensions of the KMF and RF have been linked to extension in the Andaman Sea and the Gulf of Thailand (e.g. Packham, 1993; Pigott and Sattayarak, 1993; Polachan, 1988). However, the timing and extent of deformation on the NW trending structures is still under debate (e.g. England and Houseman, 1986; Hall and Morley, 2004; Rangin et al., 1995; Searle, 2006), and recent workers have favoured processes

such as subduction rollback (Morley, 2001), lower crustal flow (Morley and Westaway, 2006), and changing intraplate stresses as a result of edge forces (Hall and Morley, 2004), as principal controls on extension in the basins, reducing the importance of large strike-slip faults in the evolution of Southeast Asia.

The KMF and RF have undoubtedly played a part in this evolution. Early work on the KMF identified a phase of brittle sinistral strike-slip deformation, based on the apparent offset of granites across the fault (Garson and Mitchell, 1970). Detailed field-based studies of fault kinematics have been notably lacking, until Intawong (2006) recognised an additional, older, ductile phase.

This paper presents new field evidence supporting these events on the KMF, and a similar change from ductile dextral to brittle sinistral shear on the larger, less well studied RF. Integrating this new field data with existing ages shows that the ductile phase pre-dates Himalayan deformation, and therefore the connection to the northern faults is more complicated than previously assumed.

2.0 Geological setting

2.1 The Thai Peninsula

The structural geology of the N-S trending Thai Peninsula is dominated by the KMF and RF: broadly linear NNE-trending strike-slip fault zones centered around elongate slivers of metamorphic fault rocks (Fig. 2). These are

bounded and overprinted by brittle strands, which are part of a population of parallel and branching sinistral faults which are localised into the two similar but discrete fault zones. The smaller KMF passes from Ko Phuket in the south towards Surat Thani in the north, while strands of the RF can be traced from Takua Pa in the south to Pran Buri in the north, crossing the peninsula entirely. A relatively undeformed block with a strike-normal width of no more than 50 km lies between the two faults.

Rocks in and around the fault zones are dominantly late Palaeozoic marine sediments deposited at mid-southern latitudes (Metcalfe, 2002, 2006). Most prominent are siliciclastic deposits of the Permo-Carboniferous Kaeng Krachan or Phuket Group, the oldest exposed rocks in the fault zone, which occupy a broad area of the central Thai Peninsula (Department of Mineral Resources, 1982). They comprise grey mudstone, siliceous shale, sandstone, and conglomeratic sequences between two and three km thick. Distinctive pebbly mudstones, interpreted as diamictites (Bunopas et al., 1991), are ubiquitous to the north of the KMF, and can be recognised even where they have been strongly deformed in the ductile shear zones. However, they rarely occur in the Permo-Carboniferous succession south of the fault zone.

Permian Ratburi Group carbonates overlie the Kaeng Krachan Group with either a locally conformable or unconformable contact (Garson et al., 1975; Bunopas et al., 1991). They are exposed as tropical tower karsts (Baird and Bosence, 1993), the long axes of which typically parallel the NNE-SSW structural trend on the peninsula. Sandstones and shales of the Jurassic to

Cretaceous Thung Yai Group crop out on the eastern side of the RF, and all lithologies are progressively overlain by Quaternary deposits as topographic relief decreases towards the Gulf of Thailand (Department of Mineral Resources, 1982, 2006).

2.2 Regional context

The Thai Peninsula lies near the western edge of Sundaland, the southeastern promontory of the Eurasia plate which is bounded by active oceanic spreading centres, strike-slip faults, and pre-Cenozoic sutures (Hall and Morley, 2004). Sundaland's coherence was attained in the Late Cretaceous, following a prolonged period of collision between allochthonous fragments derived from the Palaeozoic supercontinent Gondwana (e.g. Lepvrier et al., 2004; Metcalfe, 1991, 1996, 2006). Four major terranes make up mainland Southeast Asia. These are South China, Indochina, East Malaya, and Sibumasu (Metcalfe, 1991), within which the KMF and RF have formed. Additionally, several smaller terranes, including the West Burma and West Sumatra blocks, a continental fragment below East Java, and the fragments that form the Mawgyi and Woyla nappes are interpreted to have accreted to the western and southern edges of Sundaland during the Mesozoic (e.g. Barber, 2000; Metcalfe, 1996; Mitchell, 1993; Smyth et al., 2007).

Magmatism attributed to this prolonged phase of subduction, collision and crustal thickening occurred across eastern Myanmar, western Thailand, peninsular Malaysia and Sumatra. Granitoids rich in ore deposits occur as stocks and N-S trending elongate batholiths, arranged into three

geochronologically and petrologically distinct N-S trending bands: the Western, Main Range, and Eastern Granite Provinces (e.g. Charusiri, 1989; Cobbing et al., 1986; Hutchison, 1989; Putthapiban and Schwartz, 1994; Ridd, 1978). The granites range from small I-type Permo-Triassic intrusions in the east to larger S-type Palaeogene bodies in the west (Charusiri, 1989; Cobbing et al., 1986; Putthapiban and Schwartz, 1994). Granites of the Western Province lie within and around the KMF and RF, while Main Range granites crop out immediately SE of the KMF (Fig. 1 and Fig. 2).

3.0 Deformation on the Khlong Marui and Ranong Faults

Satellite imagery clearly reveals the position, orientation and scale of deformation across the fault zones, and reports of granites across the peninsula have alluded to fabrics attributed to strike-slip shear (e.g. Charusiri, 1989, Hutchison, 1989; Nakapadungrat et al., 1991; Putthapiban, 1992). The faults have consequently been included in models for the Tertiary tectonic evolution of Southeast Asia, including those of Tapponnier (1986), Lee and Lawver (1995), Hall (1996, 2002), and Replumaz and Tapponnier (2003), typically acting as a boundary between fragments representing the northern and southern parts of the Thai-Malay Peninsula. Displacement estimates have ranged from 100 km of dextral offset on the KMF (Kornsawan and Morley, 2002) to at least 200 km of sinistral offset (Garson and Mitchell, 1970); and from 200 km (Tapponnier et al., 1986) of dextral offset on the RF, to 20 km of sinistral offset (Garson and Mitchell, 1970). Ridd's (1978) estimate of combined sinistral displacement on the KMF and Kapoe Fault (part of the RF) was 250 km. The

158 timing of the dextral displacements is typically modeled according to the faults'
159 hypothesised role as conjugate structures to the MPF and TPF, which were
160 sinistral in the Oligocene (Lacassin et al., 1997). Recent field studies have
161 shown that the KMF has experienced a change from ductile dextral to brittle
162 sinistral strike-slip motion (Intawong, 2006), as has long been assumed. This
163 paper demonstrates a similar change on the RF, and constraints on the timing of
164 deformation phases across the whole of the KMF and RF.

165 The fault zones were mapped using a combination of detailed fieldwork
166 in Thailand, 30 metre Landsat TM multi-spectral imagery and 90 metre Shuttle
167 Radar Topography Mission (SRTM) Version 2 data for Thailand and Myanmar,
168 1/250,000 scale aeromagnetic anomaly maps and Th, U, and total count
169 radiation maps for Thailand. Sedimentary and intrusive rocks outside the fault
170 zone shown on the fault maps are modified from 1/50,000 and 1/250,000 scale
171 maps published by the Thai Department of Mineral Resources (1980, 1982,
172 1992, 2006). Four phases of strike-slip deformation were identified (D_1, D_2, D_3,
173 and D_4), which have similar orientation and expression in both fault zones.
174

175 *3.1 D_1*

176 Deformation phase 1 involved dominantly non-coaxial dextral strike-
177 slip strain at low metamorphic grades, followed by folding of variable intensity.
178 It is recorded by pelites and metaconglomerates of the Kaeng Krachan Group
179 with a continuous cleavage or domainal spaced cleavage S_1 which strikes
180 between 000° and 035° and dips variably to the east and west. Original

sedimentary bedding S_0 is rarely discernable. A prominent lineation on S_1 typically plunges less than 20° and is defined by mica elongation and stretched clasts.

Fine grained micas define S_1, which flows smoothly around porphyroclasts of quartz, lithic fragments of sandstone and more rarely mudstone (Fig. 3a). Euhedral apatite within some quartz clasts indicates that they are derived directly from an igneous parent rock. Smaller quartz clasts are monocrystalline, with undulose extinction in random orientations, probably a record of pre-sedimentary deformation. Dissolution away from angular porphyroclast corners is expressed by rounding and seams of opaque insoluble material which form strain caps and enhance S_1. The fabric varies from cataclastic to mylonitic, and strain is rather variable. While matrix quartz typically does not show evidence of dynamic recrystallisation, zones of bulging and subgrain rotation recrystallisation are locally developed. Diffuse pressure shadows, formed by very small grains of recrystallised quartz and mica concentrations, are common around larger porphyroclasts and relict pebbles in areas of higher strain.

Asymmetric elongation of porphyroclasts, stair-stepping pressure shadows and mica fish indicate consistently dextral shear coeval with S_1 development. Rare C-S fabrics defined by superposition of dark dissolution seams on older S planes formed by mica alignment record the same shear sense.

Folding of S_1 is highly variable, but typically involves asymmetric harmonic parallel and chevron folds and kink bands (Fig. 3b). These have axial

surfaces which dip to the SE, SW and N, and hinge lines which plunge moderately to the NW, NE and W. Folds develop on all scales including microscopic, but no secondary cleavage is associated with them. The style and orientation of folding shows that it occurred during a late stage of D_1, at lower metamorphic conditions than strike-slip deformation.

Structural relationships indicating that D_1 is the first deformation event on the KMF and RF are unambiguous only at Ranong (Fig. 4). A well defined band of sheared and folded rocks are obliquely cut by the Ranong granite, which is itself cut by a younger, medium grade shear zone, attributed to D_2. At a number of other locations on the RF, similar fault rocks are intruded by dykes of the same latest Cretaceous age as the Ranong granite. Other areas interpreted to record D_1 deformation, including those within the KMF, have been mapped based on the distinctive deformation style which is similar to that of the sheared and folded rocks at Ranong. While it is likely that D_2 overprinted much of the D_1 shear zone, its intensity and duration were such that older fabrics in areas of D_2 deformation cannot be confidently attributed to D_1.

3.2 D_2

The most intense phase of deformation, D_2, was a period of non-coaxial dextral strike-slip strain at medium to high metamorphic grades. Rocks deformed by D_2 are exposed within at least five elongate slivers of metamorphic rocks on the RF, while on the KMF, a single sliver is exposed (Fig. 2). D_2 formed a widespread foliation S_2 which strikes 005° to 030° and

dips both east and west at angles greater than 50°. Mineral stretching lineations developed on these planes plunge at a shallow angle to the NNE and SSW.

Five broad metamorphic lithologies were created by, or modified during deformation associated with D_2. These are, in order of prevalence: poorly segregated, high melt migmatites; foliated granites and orthogneisses; well segregated, low melt migmatites; quartz-biotite mylonites; and a range of sheared meta-sediments.

3.2.1 High melt volume migmatite

High melt volume stromatic and nebulitic migmatites (Fig. 3c) are limited to the RF, and crop out discontinuously in two strands between Kra Buri and Bang Saphan (Fig. 5 and Fig. 6). They differ from the low melt migmatites not just in anatexis magnitude, but in mesosome texture. Mesosomes are medium grey in colour, coarser grained, contain more biotite and have a less schistose, more gneissic foliation. They contain finely disseminated leucocratic material, including isolated, large, well rounded K-feldspar phenocrysts with recrystallised feldspar and quartz sigma-type strain shadows. This indicates temperatures during shear above the brittle – crystalplastic transition for feldspar in wet rocks (~500°C) (Gapais, 1989; Passchier and Trouw, 2005). Leucosomes are typically wispy, poorly defined, and rarely bounded by melanosomes. K-feldspar and plagioclase again show evidence of crystalplastic flow, and there is extensive grain boundary migration in quartz crystals. Hornblende and garnet are commonly present, and deform by

brittle mechanisms, indicating temperatures during shearing below 700 °C. Synthetic dextral shear bands between leucosome boudins are common.

3.2.2 Foliated granites and orthogneisses

The high melt volume migmatites always have a close spatial association with foliated granites. Deformation of the granites occurred under a range of metamorphic conditions, commonly within the greenschist facies. Locally pervasive S-C' fabrics illustrate progressive retrograde metamorphism during shearing in some of the foliated granites (Fig. 3d). Original S-planes are defined by foliation-parallel bands of coarse biotite which curve around deformed feldspar porphyroclasts. Feldspars deform in a brittle manner, expressed by micro- and macroscopic sinistral domino-style antithetic faults in subhedral K-feldspar phenocrysts, by microscopic tectonic abrasion of all feldspars, and by bent plagioclase twin lamellae. Recrystallised quartz shows undulose extinction, and is typically arranged into elongate polycrystalline aggregates, ribbons and tails emanating from rounded feldspar porphyroclasts. These structures display a clear dextral stair-stepping geometry at all scales of observation. Regular, closely spaced dextral C' planes reveal continued shearing under cooler conditions. They are dominated by small quartz grains formed by bulging recrystallisation, chlorite, clastic fragments of feldspar, euhedral zircons, and fine biotite fragments. Quartz was ductile in both of these phases, indicating temperatures not below ~ 300°C (Stipp et al., 2002) during all of the deformation associated with D_2, a conclusion common to all of the rocks deformed during D_2.

Biotite is not a major component of the interfolial domains, taken to represent protolith composition, so the large biotite crystals partly defining S-planes are interpreted to be syn-kinematic in origin, rather than reoriented magmatic crystals. The finely crushed mica in C'-planes probably originated in the S-planes, suggesting that no new biotite growth occurred during this younger period of deformation.

Crystalplastic deformation, deformation twins and subgrain development in feldspar porphyroclasts occurs in regions of higher grade metamorphism, together with extensive myrmekite, quartz grain boundary migration, and biotite rich pressure shadows. In some granites, S-C' fabrics do not record significant retrograde metamorphism, most notably near Khao Nakkharat, northwest of Bang Saphan. The younger C' planes here are defined by fine grained quartz ribbons, and mantled feldspar porphyroclasts, with dextral asymmetry. These show extensive crystalplastic deformation parallel to the shear planes. Titanite is concentrated in these planes, and is the only mineral that fractures in a brittle manner. Higher grade foliated granites such as these are essentially mylonitic orthogneisses, with S_2 expressed by crude segregation of quartzo-feldspathic and mafic minerals, or extreme elongation of feldspar grains in L-tectonites.

3.2.3 Low melt volume migmatites

Kilometre-scale bands of low melt volume stromatic or ophthalmic migmatites are commonly in faulted contact with quartz biotite mylonites. They are best developed on the RF close to the Myanmar border north of Ban Pak

295 Chan (Fig. 5), within the isolated ductile core north of Kapoe, and on the
296 eastern side of Khao Phanom, the KMF ductile core (Fig. 7). The mesosome of
297 these migmatites is compositionally similar to the mylonites, but foliation-
298 parallel biotite is more coarse grained, and clots of fibrolitic sillimanite suggest
299 that the migmatite is a higher grade development of the mylonite. A spaced
300 schistosity is defined by biotite domains and quartzo-feldspathic microlithons.
301 A fine biotite mineral lineation marks foliation surfaces.

302 Sigma-type quartz lenses are well developed within the mesosome, and
303 contain significant amounts of K-feldspar and euhedral hornblende. These are
304 compositionally similar to coarse microlithons, and indicate a progression from
305 quartz-biotite segregation in the mylonites, to more complete mafic-felsic
306 segregation and incipient melting. Larger leucosomes have the same
307 composition, but are coarser, more feldspathic, and possess a variably
308 developed foliation defined by hornblende and elongate quartz shape preferred
309 orientation. They are also surrounded by dark, felsic depleted melanosomes,
310 indicating local melt derivation. Fully developed leucosomes range in thickness
311 from 1 cm to 2 m, and form sheet-like bodies parallel to S_2, but rarely comprise
312 more than 20 % of the total rock volume. The contact between the two
313 components is usually sharp, but locally diffuse.

314 In all cases the leucosomes are necked, and often form well-spaced
315 ellipsoidal ductile boudins (Fig. 3e). Extensional shears with a dextral
316 asymmetry form between boudins at angles less than 30° to the tectonic fabric;
317 these are thus interpreted as synthetic shear bands. More rarely, boudins are

separated by antithetic shear bands with a sinistral shear sense. In both instances, the host foliation flows smoothly around the pinch and swell structures, and the shear bands curve into parallelism with the foliation immediately outside the leucosome. Since formation of the mesosome schistosity is interpreted to be coeval with D_2 dextral shear, and leucosomes form parallel to this fabric and also record dextral deformation in the same orientation, it can be inferred that migmatisation was syn-kinematic with respect to D_2.

3.2.4 Quartz-biotite mylonites

Quartz-biotite mylonites form broad bands of fairly homogeneous deformation. They have a similar composition to the low melt volume migmatites, but all minerals are finer, the foliation is more continuous and microlithons are thin and composed entirely of quartz. Sillimanite and melt lenses are absent. Faint colour and compositional banding parallel to S_2 may be the remnants of sedimentary bedding in the protolith, while lithic clasts of granite, quartzite and quartz flattened parallel to S_2 and stretched parallel to the mineral lineation also attest to a sedimentary origin. Lithic clasts are present in a more deformed state in the low melt volume migmatite. Their size, composition and distribution in a bedded, fine grained silicic rock indicates that the protolith for both lithologies may be the pebbly mudstones of the Kaeng Krachan Group, which are found in an un-deformed state adjacent to both faults. Deposition of the Kaeng Krachan Group ended in the Lower Permian

(e.g. Bunopas et al., 1991; Fujikawa et al., 2005), placing a maximum age limit on the onset of D_2.

The long axes of deformed sedimentary clasts are rotated anti-clockwise relative to the foliation in horizontal section, forming a dextral stair-stepping geometry augmented by crystal-plastic quartz mantles. Similar sigma-type quartz objects without obvious cores form foliation-parallel asymmetric ductile boudin trails. These may be pre-metamorphism quartz veins rotated or transposed into parallelism with the foliation. However, grain sizes and sub-grain rotation patterns in the boudins are identical to grains in microlithons between biotite rich domains, indicating that they formed by the same processes, perhaps as a stage towards a more gneissic segregation. It is interesting to note that the vast majority of asymmetric objects are sigma-type; delta-type objects are rare, especially in the KMF. This may indicate low strain rates, as the embayments typical of delta-type objects can be filled by recrystallised material before the object has rotated further during low strain (Passchier and Simpson, 1986).

Other dextral shear sense indicators in both the mylonite and low melt migmatite include S-C' fabrics, mica fish and asymmetric folds. Folding during D_2 was less well developed than during D_1, but always had a ductile nature, and formed long amplitude, short wavelength structures with dextral vergence. Three broad fold styles are characteristic. The first is harmonic similar folding of S_2 which is common in more homogeneous quartz-biotite mylonites. Axial planes are subparallel to S_2, and hinge lines appear to be orthogonal to the

ductile lineation. It is likely that these represent oblique sections through the noses of tubular sheath folds. Structurally similar folds affect high melt volume migmatites along Huai Chang Raek, SW of Bang Saphan Noi (Fig. 2 and Fig. 6). These also have steeply plunging hinge lines, but their axial planes strike ~ 150°, oblique to the foliation and migmatitic segregation. Structures indicating high grade dextral shear flow around the folds, and leucosome bands are transposed into parallelism with fold axes, and into discontinuous bands striking ~050° where short limbs are highly thinned. These are interpreted to be late D_2 folds formed during retrograde metamorphism, and are synchronous with low grade S-C' fabrics in the foliated granites. The third fold style occurs in the low melt migmatites. Thin leucosomes can display disharmonic ptygmatic and rootless folds (Fig. 3f), and therefore indicate continued ductile deformation after melt segregation. All folds are coeval with D_2.

3.3 D_3

D_3 is characterised by a period of sinistral strike-slip faulting, marked at the surface by steeply dipping faults with a wide range of orientations, but dominantly between 000° and 030°. Most of the Thai Peninsula between Phuket and Pran Buri is intensely cut by an anastomosing network of these structures (Fig. 2). They occur both within and outside the D_1-D_2 ductile cores, and within the central, most densely faulted region, divergent branches re-link to form elongate wedges containing metamorphic rocks in abrupt contact with unsheared sedimentary rocks. Steep, linear valleys and elongate karstic mountains are the characteristic geomorphic expression of these structures (Fig.

8a), so they can be traced from satellite imagery. A swathe of faults on the RF is 440 km long and up to 50 km wide, though individual strands are rarely longer than 150 km. Combined with a ~200 km projection offshore into the Mergui Basin (Intawong, 2006; Polachan, 1988), the total brittle length of the RF may be between 500 and 650 km. Onshore faults are concentrated on the Thai side of the border, with fewer, but longer and more deeply incised fault valleys in Myanmar. To the west of the main population, the strands start to curve to the north and NW, where they enter the Andaman Sea near Mergui.

The KMF has a much simpler expression, with only about six major strands, all of which have very clear topographic expression, defining a fault zone 210 km long and 25 km wide. A number of short, parallel faults exist within the relatively undeformed block between the RF and KMF, which has a width no more than 50 km normal to the structural trend. Fault density decreases towards the east of the peninsula on both faults, though it is possible that structures exist in this area and are hidden by Quaternary deposits. Strands at the northeastern end of both fault zones appear to curve northward before disappearing.

Outcrops of major fault strands are characterised by zones of cataclasis tens of metres wide, mostly composed of coarse, poorly sorted, angular clasts set in a matrix of finer breccia, unfoliated gouge or quartz (Fig. 8b). Within these zones, narrow, anastomosing bands of high strain contain fine breccia, foliated gouge and discrete fault planes with slickensides. Several generations

of high strain bands are often present within a single major D_3 strand, which record a complex history of overprinting and reactivation.

Breccia zones between unsheared sediments and high grade metamorphic rocks are made up of fragments of both lithologies, which are increasingly mixed and rotated away from their original orientation towards the centre of the breccia zone. Clast shapes include nested duplex-like stacks of orthorhombic slivers, and more equant fragments. Within at least two fault strands on the RF, unfoliated felsite veins injected into an early fault breccia have cooled and subsequently been sliced into angular blocks themselves by narrow, chlorite-rich faults. A similar process may account for the more common quartz breccias composed of clasts of an older quartz breccia together with fragments of host rock. At the margin of breccia bands the host rock is often intensely fractured and veined, with small discrete faults in all orientations forming a broad damage zone.

Large, discrete fault planes exist both within the cataclasis zone of major brittle strands, and as isolated minor structures in intact rock. They are often polished and marked by slickensides which indicate either pure strike-slip, or oblique-slip movement. In the latter case, slickensides plunge up to 50° to the NE or SW. More rarely, two or more generations of slickensides are present on the same plane, with the oldest almost always sub-horizontal. Fault plane steps are usually ambiguous, but tend to indicate sinistral motion, or reverse sinistral where they are oblique. Small contractional duplexes in oblique damage zones also indicate reverse oblique sinistral shear. Occasional normal

overprinting of the reverse sinistral fabrics indicates localised extension during the late stages of, or after, D_3 (Fig. 8c).

The contrast between neighbouring rocks on either side of D_3 faults is sometimes extreme. For example, the biotite-sillimanite low melt migmatites of the KMF exposed on the eastern side of Khao Phanom occur within 3.5 km of undeformed limestones of the Ratburi Group (Fig. 7). The actual contact is obscured by alluvium, and may be much closer. Contacts on the east side of the western RF D_2 strand NW of Chumphon are even more abrupt. High melt volume migmatites and amphibolite facies granite mylonites crop out within 50 m of pebbly mudstones of the Kaeng Krachan Group and Jurassic red-beds (Fig. 5), neither of which shows any evidence of homogeneous strain, contact or regional metamorphism. This implies significant vertical movement. There is no evidence of large scale thrusting, and 83 % of 368 measured D_3 fault planes have dips $\geq 45°$.

Absolute displacement of individual fault strands is usually unclear, as most lithological boundaries are parallel to the faults. Where there is obliquity, however, a minimum estimate can be made. For example, the Ranong granite is obliquely truncated by a dextral D_2 shear zone, but part of the deformed northern tip of the granite has a present-day sinistral offset relative to the main body of at least 10 km along three D_3 strands (Fig. 4). Displacements visible in the field are in the order of decimetres (Fig. 8d), proportional to the reduced width of the individual faults. The total displacement on the fault zones must be the sum of individual displacements on major strands. If the Ranong example is

typical, an average sinistral slip of about 3.3 km may characterise the main strands. The RF is composed of at least 25 major D_3 strands, yielding an estimated displacement of about 80 km. The KMF has fewer strands, and displacement may be of the order of 20 km.

3.4 D_4

The least intense phase of deformation, D_4 was a period of brittle dextral strike-slip faulting. It is expressed by outcrop scale strike-slip fault arrays which are pervasive across the KMF and RF, and cut across the metamorphic cores and D_3 fault zones. The faults are typically discrete, planar surfaces less than 10 m long, and often just several centimetres long. Thin bands of gouge are developed only on the larger through-going faults. Features such as R (Fig. 8e) and R' Riedel shears, P-shears, releasing bends and horsetail splays are well developed and typically indicate dominant dextral displacement (Fig. 9). These structures strike between 050° and 120°, and so are commonly at a high oblique angle to the older fabrics (Fig. 9). They have vertical to very steep dips.

Shear sense and amount are usually clear because of this obliquity. Markers such as migmatite leucosome bands and quartz segregations in mylonites are cleanly deflected, show little folding into the faults, and are not altered by fault fluids (Fig. 8f). Dextral displacement is typically 0.5 to 10 cm on individual faults, but can be an order of magnitude higher across well developed arrays. Antithetic sinistral faults are locally observed at about 45° clockwise from the main array, though these are subordinate in length and displacement (Fig. 9). Mineral precipitation is limited to rare quartz crystals

which indicate strike-normal extension, perhaps during a later dilatational phase. In one region within the KMF ductile core, space generated by horsetail splays at the ends of D_4 faults has been intruded by a quartzo-feldspathic fluid which may have a magmatic origin, and would be the youngest such intrusion in the fault zone.

Remote sensing data indicate that kilometre-scale faults with similar orientations cross cut the major sinistral faults, and very occasionally show topographic dextral displacements. It is possible that these are the main foci of D_4 strain, and the outcrop faults simply represent dissipation of this strain within fault-bounded blocks.

4.0 Timing of fault activity and magmatism

4.1 Timing of D_1 and D_2

While there are no isotopic age data from the mylonites and migmatites on either fault, a considerable number of dates exist in the literature for the granitoid plutons, stocks, dykes and associated pegmatites which lie along the faults' traces throughout the Thai Peninsula. Their petrology and geochronology have been extensively studied, principally because they host globally important reserves of tin (e.g. Bignell, 1972; Charusiri, 1989; Cobbing et al., 1986; Hutchison, 1989; Putthapiban and Schwartz, 1994; Schwartz et al., 1995). It is informative to put these data into the context of the KMF and RF deformation history presented here.

Where intrusions interact with the fault zones, they can be classified as pre-, syn-, or post-kinematic with respect to each deformation phase. No intrusions in the fault zones can be shown to be pre-kinematic with respect to D_1, while only two are unequivocally pre-kinematic with respect to D_2, both on the RF. These are the Ranong (Fig. 4) and Khao Wang Tal (Fig. 6) granites, which are cut by major ductile shear zones, and a gradient is exposed across strike from the undeformed intrusion into the sheared rocks. In addition to these intrusions, brittle fault-bounded granites in the region of retrograde S-C' fabric development west of Tha Sae show inhomogeneous deformation, with narrow, S-fabric parallel high strain ultramylonite bands. Such a feature is characteristic of deformation of pre-kinematic material (Gapais, 1989).

The Ranong granite (Fig. 4) is of particular importance because of its clear cross-cutting relationships with D_1 and D_2. A band of D_1 sheared meta-sediments extends from east of Ban Pak Chan to Ko Son, SSW of Ranong. It is obliquely cut at about 10° 5' N by the Ranong granite, a 45 km long, N-S trending coarse grained porphyritic biotite ± muscovite intrusion. Its euhedral K-feldspar phenocrysts have a fairly constant grain shape preferred orientation parallel to the intrusion's long axis, but there is no evidence of strike-slip motion during its emplacement. The NNE striking meta-sediment band continues undeflected across both sides of the intrusion, and its contact with the granite appears not to be faulted, supporting our interpretation that the Ranong Granite was intruded into the meta-sediments, and therefore post-dates D_1.

The northwestern end of the intrusion is abruptly truncated by an oblique 3.5 km wide ductile shear zone of granite mylonite and low melt volume migmatite, which extends offshore into the Mae Nam Kra Buri estuary / Andaman Sea. Both lithologies contain abundant dextral shear sense indicators as described in section 3.2. There is a steep, but apparently continuous deformation gradient from the undeformed pluton into the shear zone. Quartz develops progressively more bulging recrystallisation and chlorite is present, while further into the shear zone sub-grain rotation dominates and biotite is the principal phyllosilicate. Within the fully developed mylonites in the centre of the shear zone, quartz deforms by grain boundary migration, and feldspar begins to be recrystallised.

This shear zone is characteristic of the higher grade metamorphic fault rocks across the KMF and RF, and since it cuts the Ranong granite, which itself post-dates D_1, it is assigned to D_2. Charusiri (1989) used Ar-Ar thermochronology on mica separates to date emplacement of a leucogranite within the Ranong Granite, and Sn-W mineralisation outside the main intrusion. He concluded that these events occurred between 82 and 77 Ma. Although less reliable, Charusiri's (1989) reassessment of Bignell's (1972) whole rock Rb-Sr data for the undeformed parts of the Ranong Granite yields an age of 87 Ma, lending some support to a Late Cretaceous age to the body. This age means D_1 must have concluded by the mid Late Cretaceous, and D_2 must have started after this time.

Bignell (1972) used the K-Ar method to date muscovite from a foliated biotite – muscovite granite at Ban Set Takuat (Fig. 4), within the D_2 shear zone which truncates the Ranong granite, to propose a cooling age of 68.1 Ma. It has been shown above that dextral shear ceased before the rocks cooled below the field of bulging dynamic recrystallisation for quartz (~ 300°C) (Stipp et al., 2002). Since the K-Ar closure temperature for muscovite is 350 ± 50 °C (Hames and Bowring, 1994), Bignell's (1972) age can be interpreted as cooling after D_2 metamorphism, which was sufficiently hot to have reset older magmatic mica geochronometers. The K-Ar method is now regarded unreliable in such applications, but this is the only date from the metamorphic rocks of either fault zone. It is considerably younger than the inferred age of the granite, consistent with field relationships which indicate that the Ranong Granite is pre-kinematic with respect to D_2.

Northwest of Bang Saphan Noi (Fig. 6), a NNE-trending unfoliated pegmatite dyke intruded into a sliver of rocks displaying characteristic D_1 fabrics yielded a muscovite Ar-Ar age of 71.77 ± 0.55 Ma (Charusiri, 1989). This is interpreted to date the D_1-D_2 inter-kinematic magmatism which includes the Ranong granite, and other undated intrusions which display the same field relationships.

In many cases, foliated granites and orthogneisses interpreted to have been deformed during D_2 are found only within the exhumed metamorphic cores, and so it is not clear whether they are pre- or syn-kinematic. D_2 across the KMF and RF represents a prolonged phase of metamorphism and

565 migmatisation in one or more ductile shear zones which may penetrate to a
566 considerable depth in the lithosphere. Magmatism commonly occurs in such
567 settings because of the close link between conditions of tectonic deformation
568 and granite melting (Druguet and Hutton, 1998; Hutton, 1992). Intraplate
569 crustal-scale strike-slip faults which penetrate the lithospheric mantle can act as
570 continuous melt conduits (Leloup et al., 1995), and focus magmatic generation,
571 ascent and emplacement (Hutton, 1988; Hutton and Reavy, 1992). Examples of
572 high strain shear zones which contain syn-kinematic intrusions include the
573 TIPA shear zone, Argentina (Höckenreiner et al., 2003), the Main Donegal
574 Shear Zone, Ireland, (Hutton, 1982), and the Closepet granite, southern India
575 (Moyen et al., 2003). On this basis it might be expected that some of the
576 foliated granites in the KMF and RF are syn-kinematic with respect to D_2. The
577 criteria of Searle (2006) can be used to help determine whether this is the case.
578
579 The following features indicate a syn-kinematic origin:
580
581 1.) Based on field evidence and remote sensing data, none of the sheared
582 granites (with the exception of the Ranong and Khao Wang Tal
583 granites) can be traced outside the ductile fault zones.
584 2.) Where a more complete ductile strand is exposed, for example the area
585 around Khao Plai Khlong Hin Phao within the RF (Fig. 5), there is a
586 gradient from sheared granite in the east, to high then low melt volume
587 migmatite, then lower grade quartz-biotite mylonites in the west, despite

disruption from younger faults. A similar pattern occurs across the KMF ductile core (Fig. 7). Although this sequence is not exposed in all parts of the faults, high grade metamorphic rocks occur along the whole length of the exposed ductile cores. This indicates a close spatial and dynamic link between migmatisation, syn-tectonic intrusions and high grade metamorphism.

3.) *In situ* melting occurs in all of these areas, and all leucosomes are affected to a greater or lesser extent by shearing, with the development of foliations and mineral lineations. Shear sense and orientation are the same in both components of migmatites and in sheared granites.

4.) Migmatite xenoliths are common in the weakly foliated granite of the KMF ductile core.

5.) Large granitic bodies within the migmatite zone of the KMF ductile core display a notably broad spectrum of deformation intensity over a narrow area. Fabrics range from magmatic to sub-magmatic hornblende mica and feldspar lineations, to well developed metamorphic mica foliations and crystal-plastic feldspar deformation. This variation may reflect variable strain as a result of being emplaced at different times during D_2.

6.) Late stage pegmatite dykes within foliated granites typically record lower levels of strain than their host rocks.

These criteria suggest that some of the foliated granites in the KMF and RF formed during D_2, possibly related to partial melting associated with formation of the western province granites. There are presently no age data from any of the foliated bodies.

Intrusive bodies which are post-kinematic with respect to D_2 lie along the central section of the RF. A suite of irregularly shaped porphyritic biotite-muscovite granite intrusions west of Bang Saphan Noi lie wholly within a 5 km wide sliver of high melt volume migmatite (Fig. 6), but show no evidence of solid state ductile deformation. An equally undeformed intrusion along the high ridge of Khao Plai Khlong Hin Phao (Fig. 5), west of Tha Sae, is broadly parallel to the ductile fabric of the mylonites it intrudes, but its contacts locally cross cut it. Neither deflection of the ductile fabric, nor systematic variation in country rock composition and texture is observed as a function of proximity to the intrusions. The granite – country rock contact is locally faulted by narrow brittle faults and thin, low grade mylonite zones, but the primary contact is interpreted to be intrusive. Most critical to this interpretation is the presence of small xenoliths of granitic ultramylonite within the pluton. A large, irregularly shaped migmatite xenolith found within one of the plutons west of Bang Saphan Noi also supports the conclusion that these granites post-date D_2 deformation, and are not low strain enclaves of pre-kinematic basement surrounded by anastomosing high strain shear zones.

None of the bodies which intrude exposed D_2 metamorphic cores have been dated. However, a biotite separate from a medium grained biotite ± muscovite granite NW of Thap Sakae was dated by Charusiri (1989), using the Ar-Ar method, at 53.24 ± 0.71 Ma; and by Bignell (1972) using the K-Ar method, also on a biotite separate, at 51.8 Ma. The intrusion is compositionally and texturally similar to nearby intrusions within the migmatites. If these bodies were emplaced at the same time, as part of the fault controlled early Eocene magmatism proposed by Charusiri (1989), they indicate that D_2 on the RF terminated before about 54 Ma.

The Khao Lak granite, 12 km west of the KMF ductile strand, is hosted mostly by Permo-Carboniferous siliciclastics, yet contains large xenoliths of migmatitic mylonite. This indicates that there are ductile fault rocks at depth which have not been exhumed, through which the granite passed during its ascent; and secondly, that the granite is post-kinematic with respect to D_2. Charusiri (1989) determined a muscovite Ar-Ar total fusion age of 55.65 ± 0.49 Ma for pegmatites within this body. Near Nam Tok Bang Thao Mae, within the KMF ductile core (Fig. 7), muscovite from an undeformed pegmatite vein which cuts D_2 mylonitic foliation yields a clear Ar-Ar plateau age of 41.32 ± 0.17 Ma (Charusiri, 1989). These results confirm that Eocene post-D_2 magmatism affected the KMF as well as the RF, and that D_2 must have ended before latest Paleocene to early Eocene times (~ 56 to 52 Ma) on both faults.

4.2 Timing of D_3 and D_4

It has been shown that metamorphic cores deformed by D_1 and D_2 are bounded, cut, and probably exhumed by D_3 brittle faults. The onset of D_3 therefore post-dates the latest Paleocene to early Eocene (~56 to 52 Ma) termination of D_2. Brittle faults assigned to D_3 on the basis of their scale, orientation and topographic expression also cut all post D_2 granites (with the possible exception of the Bang Thao Mae pegmatite). In addition to the 56 to 52 Ma ages for these rocks reviewed in section 4.1, a suite of I – and S – type granites in the Ko Phuket – Phang Nga area yield mica Ar-Ar ages of 58-55 Ma (late Paleocene to earliest Eocene) (Charusiri, 1989). Although they do not cross D_1-D_2 structures, they are clearly deformed by at least two major D_3 faults, and several smaller brittle structures (Fig. 2). The consistent ages of granites pre-kinematic with respect to D_3 across the KMF and RF indicates that D_3 began after the early Eocene (~ 52 Ma).

The offshore tectonic record can help to reinforce the constraints on fault timing established above. Numerous Tertiary basins exist east of the peninsula (Gulf of Thailand) and to the west (Andaman Sea), together with a number of small onshore basins (Fig. 1and Fig. 2). Their relationship to movement on the KMF and RF is widely disputed. Models which show the basins as pull-aparts between pairs of strike-slip faults include those of Polachan et al. (1991) and Tapponnier et al. (1982). These models invoke Himalayan lateral extrusion as the driving force behind the strike-slip faults. More recent models, including those of Westaway and Morley (2006) and Hall

and Morley (2004) propose rifting, lower crustal flow and plate edge forces as principal driving mechanisms, in which case the KMF and RF act as accommodation structures under regional extension (Intawong, 2006).

In the Gulf of Thailand, four main basins are formed by N-S trending grabens and half grabens (Polachan et al., 1991). From west to east, these are the Chumphon, Western, Kra and Pattani Basins, while the Cambodian Khmer Basin and the larger Malay Basin lie to the east and southeast respectively. Between 4 and 8 km of poorly dated terrestrial sediments fill these basins. Estimates of the ages of the oldest sediments vary from Eocene to Oligocene age, and the basins experienced subsidence rates almost an order of magnitude greater than rift basins in the North Sea, and have high present day heat flow (Hall and Morley, 2004).

A series of N-S trending grabens and half grabens form the Mergui Basin at the south western end of the RF. The fault forms the northern boundary of, and dies out west of the Ranong Trough, the eastern-most graben in the Mergui basin (Polachan, 1988). This is about 200 km along strike from where the RF passes offshore near Takua Pa. Up to 8 km of sediments fill the deepest parts of the basin, with syn-rift sedimentation beginning in the Late Oligocene (Polachan, 1988), Early Oligocene (Andreason et al., 1997), or Late Eocene (Mahattanachai, pers. comm., 2007).

Onshore, the N-S trending Khien Sa and Krabi Basins (Fig. 2) lie south of the KMF. Mammalian fossils, including primates, found in the lowest levels of the Krabi Basin indicate a Late Eocene age (Chaimanee et al., 1997), and

699 show that E-W extension on the Thai Peninsula was underway by 35 Ma
700 (Ducrocq et al., 1995).

701 Whilst there is a close spatial relationship between the Tertiary basins
702 and the KMF and RF, major through-going strike-slip faults are not prominent
703 on seismic data east of the peninsula (Intawong, 2006; Morley, 2001, 2002), as
704 might be expected if the basins were pull-aparts. Nor are they restricted to
705 within hypothetical horsetail splays. The N-S orientation of all the graben
706 bounding faults is, however, consistent with E-W extension, which could also
707 result in sinistral deformation on the KMF and RF. It follows that D_3 is
708 kinematically compatible with the late Eocene – Oligocene onset of syn-
709 kinematic sedimentation in N-S trending basins. This age is in accordance with
710 the middle Eocene maximum age for D_3 indicated by onshore granite
711 thermochronology.

712 A period of uplift during the latest Oligocene – earliest Miocene in the
713 Chumphon basin (Intawong, 2006) (Fig. 2) marks the end of the first, and major
714 rift phase. It can be correlated to inversion and an unconformity in the Pattani
715 Basin (Jardine, 1997), the Mergui Basin (Polachan et al., 1991), and to undated,
716 but stratigraphically similar unconformities in the onshore Krabi and Khien Sa
717 Basins (Intawong, 2006). This inversion may be linked to the dextral D_4 faults
718 which overprint all other structures on the KMF and RF. These faults formed at
719 a shallow level in the crust, which suggests that exhumation of the metamorphic
720 rocks was nearing completion by the time they formed in the latest Oligocene.

5.0 Discussion

5.1 The early formation of the KMF and RF

The work presented here shows that $D_1 – D_2$ ductile dextral deformation started before 87 Ma (late Cretaceous), the oldest date (Charusiri, 1989) from the Ranong Granite which cuts D_1 rocks and is cut by D_2 rocks. It ceased before 56 to 52 Ma (latest Paleocene to early Eocene), the ages of the granite at Thap Sakae equivalent to those which intrude RF D_2 migmatites, and the Khao Lak granite which contains xenoliths of KMF mylonites. All these intrusive bodies are also cut by the same D_3 faults which bound, cut, and probably exhume D_1-D_2 rocks.

It has previously been assumed that the KMF and RF, acting as conjugate structures to the TPF and MPF in Northern Thailand, underwent ductile dextral shear in the late Eocene, followed by brittle sinistral shear in the Miocene, as a result of lateral extrusion accompanying the India – Eurasia collision (e.g. Lacassin et al., 1997; Tapponnier et al., 1986). However, the evidence presented here means that $D_1 – D_2$, the high strain ductile phase of movement on the faults, preceded the start of the India – Eurasia collision, estimates for which include 55 Ma (Klootwijk et al., 1992), 55 Ma to 40 Ma (Molnar and Tapponnier, 1975), 54 Ma to 50 Ma (Searle et al., 1997), and 34 Ma (Aitchison et al., 2007).

Consequently, it is necessary to look elsewhere for the cause of this deformation. The TPF and MPF also have a long and complex history of deformation and exhumation, only part of which is related to India-Eurasia

collision (e.g. Morley, 2004, Morley et al., 2007). The cause of early KMF and RF deformation may also be responsible for an older history to the TPF and MPF.

5.1.1 An orogenic event in Northern Thailand

The fault zones coincide with the southern margin of a broad band of late Cretaceous to Paleocene uplift and orogenesis in Northern Thailand, Eastern Myanmar and Laos (Morley, 2004) (Fig. 10). Monazite ages from metamorphic core complex gneisses at Doi Inthanon, part of the Chiang Mai – Lincang belt in northern Thailand, record peak metamorphism between 84 ± 2 Ma and 72 ± 1 Ma (Dunning et al., 1995). To the west, the Mogok Metamorphic Belt in Myanmar is parallel to the Chiang-Mai – Lincang belt, and experienced a phase of high grade metamorphism which was complete by 59.9 ± 0.9 Ma (Searle et al., 2007). Apatite fission track ages from Northern Thailand indicate maximum burial or onset of uplift at between 70 to 50 Ma (Upton, 1999), while the Cretaceous to Eocene Western Province granites were intruded into this orogen, and their present-day distribution closely follows its position (e.g. Charusiri, 1989, Charusiri et al., 1993; Cobbing et al., 1986; Hutchison, 1989; Putthapiban and Schwartz, 1994; Ridd, 1978). Typically of S-type geochemistry, they indicate melting of sedimentary rocks in the crust during thickening (e.g. Charusiri et al., 1993; Zaw, 1990).

The complex network of strike-slip faults in Northern Thailand, which include the MPF and TPF, may have originated as part of a belt of Late Cretaceous to Paleocene transpression within the thickened crust (Morley,

2004). Whether or not it was conjugate to this early phase of strike-slip faulting, the dextral phase on the KMF and RF may have helped to accommodate the difference in shortening between the orogen in the north, and the un – thickened crust to the south (Fig. 10).

5.1.2 Possible causes of the orogenesis

While there is a clear coincidence between the position and timing of this orogenic event and dextral shear on the KMF and RF, the cause of the orogenesis is not clear. The most obvious involves the speculated West Burma Block (Mitchell, 1981). In the reconstructions of Metcalfe (1991, 1996, 2006), the West Burma Block was considered to be a continental fragment which accreted to the western edge of Sibumasu during the Late Cretaceous after the closure of the Meso-Tethys. Neogene dextral shear on the Sagaing fault and the Sumatran Fault, and 460 km of extension in the Andaman Sea had yet to occur (e.g. Curray, 2005; Curray et al., 1979; Hall,1996, 2002; Maung, 1987), meaning that the southern part of this block would have been emplaced in a NNE direction immediately west of the N-S trending KMF and RF. Such an arrangement is compatible with localised indenter tectonics and dextral shear on the faults during the Late Cretaceous (Fig. 10).

Although continental basement xenoliths have been found in volcanics under the eastern Central Basin, (Pivnik et al., 1998), there is little evidence that West Burma represents a large continental fragment. Mitchell (1993) interprets the andesites, basalts, ophiolites, serpentinites and cherts of West Burma to be an intra-oceanic arc thrust north-eastwards over the Eurasian margin as the

Mawgyi Nappe, geologically similar to and contemporaneous with the Woyla Nappe of West Sumatra. The Woyla arc was thrust north-eastwards over Western Sumatra during the mid to late Cretaceous (Cameron et al., 1980; Barber, 2000). A band of I-type granitoid intrusions from Aceh to Bandarlampung cut through the nappe and basement material, providing a minimum age of emplacement. These bodies yield K-Ar ages of 120 Ma to 75 Ma (McCourt et al., 1996), and may be correlatives of the 106 Ma to 91 Ma granodiorites and tonalites which intrude the Mawgyi Nappe (Mitchell, 1993). Although nappe emplacement would also have been associated with NNE-directed compression to the west of the KMF and RF, the ages of post-emplacement granites significantly pre-date the Northern Thailand orogenesis and D_2 deformation on the KMF and RF.

5.1.3 Subduction variation along the Sunda Trench

During the late Cretaceous, the Ceno-Tethys was being subducted northwards as India separated from Gondwana (Metcalfe, 1996; Ramana et al., 1994). Between 73 and 57 Ma, India moved rapidly northward at about 21cm/yr (Aitchison et al., 2007). However, while India progressed swiftly, Australia separated from Gondwana at a very slow rate (Besse and Courtillot, 1991; Cande and Mutter, 1982). An oceanic spreading centre dominated by dextral transform zones may have existed between about 90 and 100 °E to accommodate the differences between these regions. To its west, subduction around the Sundaland margin was active, while the trench to its east was inactive (Hall 2008, *In Press*).

There is evidence in the deep mantle tomographic model of Bijwaard et al. (1998) of such a change in subduction. A pronounced change in structure east of 95-100°E at depths below 700 km marks the termination of cold, NW-SE trending linear anomalies, interpreted by van der Voo et al. (1999) to represent subducted Tethyan oceans. East of about 100°E, these anomalies are not present. This indicates that from Late Cretaceous times, Ceno-Tethys was subducted in the Sunda Trench west of 95°E only (Hall et al., 2007).

The KMF and RF lie in the over-riding plate along the projected path of the spreading centre and transform zone between these regions (Fig. 10). Given that the timing of D_2 proposed here coincides with the end of Mesozoic subduction east of 100°E, it is possible that dextral shear stresses at the edge of the subducting slab were transferred upwards into the continental margin.

5.2 Brittle reactivation

5.2.1 Strike-slip inversion and exhumation of the ductile cores

It has been shown that the metamorphic cores exposed at the surface along the KMF and RF lie in the centre of a complex, bifurcating network of brittle D_3 faults (Fig. 2). These thick zones of intense cataclasis record dominantly strike-slip, but also significant subordinate oblique-slip shear, and bring elongate slivers of metamorphic rocks of up to amphibolite facies into contact with unmetamorphosed sediments. Some adjacent D_1-D_2 cores contain similar rocks, formed under similar metamorphic conditions, separated by brittle fault-bounded slivers of sedimentary cover. High to low strain gradients are only occasionally observed in individual cores, and regular, sinusoidal

curvature of the ductile foliation is not present, as might be expected if the cores represented individual ductile strands. Instead, the cores are interpreted simply as slices gouged out of one or more larger ductile shear zones, much of which may remain at depth, and therefore the slices do not represent the original D_1-D_2 shear zone structure. In the absence of evidence for significant thrusting, it seems likely that differential uplift on such a scale must have occurred within D_3 positive flower structures along the central part of both faults (Fig. 11). Apatite fission-track ages from the Thai Peninsula indicate a period of exhumation between 44 Ma and 20 Ma, with the majority around the Oligocene – Miocene boundary (Upton, 1999). At this time D_3 was drawing to a close, and the fission track ages may represent denudation of a topography elevated by the flower structures.

The present day fault zones are therefore a mélange of slivers from all depths, which have been translated both vertically and longitudinally by D_3 faulting. Broad uplift associated with these structures may explain the elevated topography north of the KMF and throughout the RF, and the dramatic lithological change south of the KMF.

5.2.2 Driving forces behind brittle reactivation

The age of D_3 interpreted here corresponds closely to the re-initiation of subduction on the southern part of the Sunda Trench in the Middle Eocene, marked by arc volcanism in the Southern Mountains of East Java (Smyth, 2005), and triggered by the acceleration in northward movement of Australia in the Early to Middle Eocene (Cande and Mutter, 1982; Royer and Sandwell,

1989). The oldest syn-rift sediments in many of the Tertiary basins across Sundaland were also deposited from the Middle to Late Eocene (summarised in Hall and Morley, 2004). These basins may have formed under a broad E-W extensional regime as a result of a N-S maximum horizontal stress, before active northwards subduction resumed ahead of Australia (Hall 2008, *In Press*). Thin, weak Sundaland lithosphere (Hall and Morley, 2004; Hyndman et al., 2005) rifted easily under these conditions, which were also compatible with sinistral movement on the NNE trending KMF and RF, weakened following D_1-D_2 deformation and pre-, syn- and post kinematic magmatism. It therefore seems likely that the main brittle phase of faulting was triggered by the onset of Eocene-Recent subduction zone at the southern margin of Sundaland attempted to re-activate.

6.0 Conclusions

New field data combined with existing isotopic ages for the Western Province granites in peninsular Thailand allow a tentative kinematic history for the KMF and RF to be constructed:

- The KMF and RF are zones of major strike-slip faulting divided into four phases:

  D_1 low grade ductile dextral strike-slip shear complete before 87 Ma.

  D_2 medium to high grade ductile dextral strike-slip shear after 72 Ma and before 56 Ma.

882 D_3 brittle sinistral and sinistral reverse oblique strike-slip shear
883 after 52 Ma.
884 D_4 brittle dextral strike-slip shear at about 23 Ma.

885 • Ductile dextral shear pre-dates both the India – Eurasia collision and
886 ductile sinistral shear on the MPF and TPF, to which the KMF and RF
887 had been assumed to be conjugate.
888 • They may instead have accommodated the southern margin of a band of
889 orogenesis in western Sundaland, which may be linked to cessation of
890 subduction southeast of the northern tip of Sumatra in the Late
891 Cretaceous.
892 • Eocene – Oligocene D_3 reactivation of the fault zones during regional
893 extension under a broadly N-S maximum principal stress was coeval
894 with basin development offshore, and the resumption of subduction
895 around the south of Sundaland.
896 • Onshore transpression during D_3 resulted in deep rooted positive flower
897 structures which exhumed slivers of the metamorphic shear zone.
898 • Early Miocene inversion, particularly in the Tertiary basins nearest the
899 faults, may be linked to D_4 strike-slip faulting across the fault zones.
900

901 ## Acknowledgements

902 We are grateful to the Department of Geological Sciences at Chiang Mai
903 University and the Department of Mineral Resources, Bangkok, for their
904 assistance and logistical support in the field; and to C.K. Morley for his

905 constructive review of the manuscript. This work is funded by the SE Asia
906 Research Group at Royal Holloway, University of London, supported by a
907 consortium of oil companies.
908

References

Aitchison, J.C., Ali, J.R., and Davis, A.M., 2007. When and where did India and Asia collide?. Journal of Geophysical Research 112, B05423, doi:10.1029/2006JB004706.

Andreason, M.W., Mudford, B., Onge, J.E.S., 1997. Geologic evolution and petroleum system of Thailand Andaman Sea Basins. In: Howes, J.V.C., Noble, R.A., (Eds.), Proceedings of the International Conference on Petroleum Systems of SE Asia and Australia, Indonesian Petroleum Association. pp. 337-350.

Baird, A., and Bosence, D., 1993. The sedimentological and diagenetic evolution of the Ratburi Limestone, Peninsular Thailand. Journal of Southeast Asian Earth Sciences 8, 173-180.

Barber, A.J., 2000. The origin of the Woyla Terranes in Sumatra and the Late Mesozoic evolution of the Sundaland margin. Journal of Asian Earth Sciences 18, 713-738.

Besse, J. and Courtillot, V., 1991. Revised and synthetic polar wander maps of the African, Eurasian, North American and Indian Plates, and true polar wander since 200 Ma. Journal of Geophysical Research 96, 4029-4050.

Bignell, J.D., 1972. The geochronology of the Malayan Granites. Unpublished PhD Thesis, University of Oxford, 154 pp.

Bijwaard, H., Spakman, W., and Engdahl, E.R., 1998. Closing the gap between regional and global travel time tomography. Journal of Geophysical Research 103, 30055-30078.

Briais, A., Patriat, P., and Tapponnier, P., 1993. Updated interpretation of magnetic anomalies and seafloor spreading stages in the South China Sea: Implications for

the Tertiary tectonics of Southeast Asia. Journal of Geophysical Research 98, 6299-6328.

Bunopas, S., Jungyusuk, N., and Khositanont, 1991. Summary of geology of Southern Thailand. In: Southern Thailand: Lithophile mineral deposits (Ranong – Takua Pa – Phuket), The Seventh Regional Conference on Geology, Mineral and Energy Resources of Southeast Asia and The Third Symposium IGCP 282: Rare Metal Granitoids. Geological excursion guidebook no.2, by Nakapadungrat, S., Jungyusuk, N., Putthapiban, P., Kosuwan, S., and Chaimanee, N, 1-13.

Cameron, N.R., Clarke, M.C.G., Aldiss, D.T., Aspden, J.A., Djunuddin, A., 1980. The geological evolution of North Sumatra. In: Proceedings of the Indonesian Petroleum Association, Annual Convention, 9, pp. 149– 187.

Cande, S.C., and Mutter, J.C., 1982. A revised identification of the oldest sea-floor spreading anomalies between Australia and Antarctica. Earth and Planetary Science Letters 58, 151-160.

Chaimanee, Y., Suteethorn, V., Jaeger, J-J., and Ducrocq, S., 1997. A Late Eocene anthropoid primate from Thailand. Nature 385, 429-431.

Châruṣiri, P., 1989. Lithophile Metallogenetic Epochs of Thailand: A Geological and Geochronological Investigation. Unpublished PhD Thesis, Queen's University, Kingston, Ontario, Canada, 819 pp.

Châruṣiri, P., Clark, A.H., Farrar, E., Archibald, D., and Châruṣiri, B., 1993. Granite belts in Thailand: evidence from the $^{40}Ar/^{39}Ar$ geochronological and geological syntheses. Journal of Southeast Asian Earth Sciences 8, 127-136.

954 Cobbing, E.J., Mallick, D.I.J., Pitfield, P.E.J., and Teoh, L.H., 1986. The granites of the
955 Southeast Asian Tin Belt. Journal of the Geological Society, London 143, 537-
956 550.
957 Curray, J.R., Moore, D.G., Lawver, L.A., Emmel, F.J., Raitt, R.W., Henry, M.,
958 Kieckhefer, R., 1979. Tectonics of the Andaman Sea and Burma. In: Watkins,
959 J.S., Montadert, L., Dickenson, P.W. (Eds.), Geological and Geophysical
960 Investigations of Continental Margins, American Association of Petroleum
961 Geologists, Memoir 29, pp. 189–198.
962 Curray, J.R., 2005. Tectonics and History of the Andaman Sea region. Journal of Asian
963 Earth Sciences 25, 187-232.
964 Department of Mineral Resources, 1980. Geological map of Thailand, scale 1:50,000.
965 Department of Mineral Resources, 1982. Geological map of Thailand, scale 1:250,000.
966 Department of Mineral Resources, 1992. Geological map of Thailand, scale 1:50,000.
967 Department of Mineral Resources, 2006. Geological map of Thailand, scale 1:50,000.
968 Druguet, E., and Hutton, D.H.W., 1998. Syntectonic magmatism in a mid-crustal
969 transpressional shear zone: an example from the Hercynian rocks of the eastern
970 Pyrenees. Journal of Structural Geology 20, 905-916.
971 Ducrocq, S., Chaimanee, Y., Suteethorn, V., and Jaeger, J-J., 1995. Mammalian faunas
972 and the ages of the continental Tertiary fossiliferous localities from Thailand.
973 Journal of Southeast Asian Earth Sciences 12, 65-78.
974

975 Dunning, G.R., Macdonald, A.S., and Barr, S.M., 1995. Zircon and Monazite U-Pb
976 dating of the Doi Inthanon core complex, northern Thailand: implications for
977 extension within the Indosinian Orogen. Tectonophysics 251, 197-213.
978 England, P., and Houseman, G., 1986. Finite strain calculations of continental
979 deformation 2. Comparison with the India-Asia collision zone. Journal of
980 Geophysical Research 91, 3664-3676.
981 Fujikawa, M., Ueno, K., Sardsud, A., Saengsrichan, W., Kamata, Y., and Hisada, K-i.,
982 2005. Early Permian ammonoids from the Kaeng Krachan Group of the
983 Phatthalung-Hat Yai area, southern peninsular Thailand. Journal of Asian Earth
984 Sciences 24, 739-752.
985 Gapais, D., 1989. Shear structures within deformed granites: mechanical and thermal
986 indicators. Geology 17, 1144-1147.
987 Garson, M.S., Young, B., Mitchell, A.H.G., and Tait, B.A.R., 1975. The geology of the
988 tin belt in Peninsular Thailand around Phuket, Phangnga, and Takua Pa. Overseas
989 Memoir of the Institute of Geological Sciences, 1, 112 pp.
990 Garson, M.S., and Mitchell, A.H., 1970. Transform faulting in the Thai Peninsula. Nature
991 22, 45-47.
992 Gilley, L.D., Harrison, T.M., Leloup, P.H., Ryerson, F.J., Lovera, O.M., and Wang, J-H.,
993 2003. Direct dating of left-lateral deformation along the Red River shear zone,
994 China and Vietnam. Journal of Geophysical Research 108, 2127-2148.
995 Hall, R., 1996. Reconstructing Cenozoic SE Asia. In: Hall, R., and Blundell, D., (Eds),
996 Tectonic Evolution of Southeast Asia, Geological Society Special Publication
997 106, 153-184.

998 Hall, R., 2002. Cenozoic geological and plate tectonic evolution of SE Asia and the SW
999 Pacific: computer-based reconstructions, model and animations. Journal of Asian
1000 Earth Sciences 20, 353-431.
1001 Hall, R., and Morley, C.K., 2004. Sundaland Basins, Continent-Ocean Interactions
1002 Within East Asian Marginal Seas. Geophysical Monograph Series 149, 55-85.
1003 Hall, R., van Hattum, M.W.A., Spakman, W., 2007. Impact of India-Asia collision on SE
1004 Asia: The record in Borneo. Tectonophysics, In Press.
1005 Hames, W.E., and Bowring, S.A., 1994. An empirical evaluation of the argon diffusion
1006 geometry in muscovite. Earth and Planetary Science Letters 124, 161-169.
1007 Höckenreiner, M., Söllner, F., and Miller, H., 2003. Dating the TIPA shear zone: an Early
1008 Devonian terrane Boundary between the Famatinian and Pampean systems (NW
1009 Argentina). Journal of South American Earth Sciences 16, 45-66.
1010 Hutchison, C.S., 1989. Geological Evolution of South – East Asia. Oxford Monographs
1011 on Geology and Geophysics, Oxford University Press, Oxford, UK, 368 pp.
1012 Hutton, D.H.W., 1982. A tectonic model for the emplacement of the Main Donegal
1013 Granite, NW Ireland. Journal of the Geological Society, London 139, 615-631.
1014 Hutton, D.H.W., 1988. Granite emplacement and tectonic controls: inferences from
1015 deformation studies. Transactions of the Royal Society of Edinburgh Earth
1016 Sciences 79, 245-255.
1017 Hutton, D.H.W., 1992. Granite sheeted complexes: evidence for the dyking ascent
1018 mechanism. Transactions of the Royal Society of Edinburgh: Earth Sciences 83,
1019 377-382.

1020 Hutton, D.H.W., and Reavy, R.J., 1992. Strike-slip tectonics and granite petrogenesis.
1021 Tectonics 11, 960-967.
1022 Hyndman, R.D., Currie, C.A., Mazzotti, S., 2005. Subduction zone backarcs, mobile
1023 belts, and orogenic heat. GSA Today 15, 4-9.
1024 Intawong, A., 2006. The structural evolution of Tertiary sedimentary basins in Southern
1025 Thailand and their relationship to the Khlong Marui Fault. Unpublished PhD
1026 thesis, Royal Holloway, University of London, UK
1027 Jardine, E., 1997. Dual petroleum governing the prolific Pattani Basin, Offshore
1028 Thailand. Proceeding of International Conference on Stratigraphy and Tectonic
1029 Evolution of Southeast Asia and the South Pacific, Bangkok, Thailand, 525-534.
1030 Klootwijk, C.T., Gee, J.S., Peirce, J.W., Smith, G.M., and McFadden, P.L., 1992. An
1031 early India-Asia contact; palaeomagnetic constraints from Ninetyeast Ridge, ODP
1032 Leg 121; with Suppl. Data 92-15. Geology 20, 395-398.
1033 Kornsawan, A., and Morley, C.K., 2002. The origin and evolution of complex transfer
1034 zones (graben shifts) in conjugate fault systems around the Funan Field, Pattani
1035 Basin, Gulf of Thailand. Journal of Structural Geology 24, 435-449.
1036 Lacassin, R., Maluski, H., Leloup, P.H., Tapponnier, P., Hinthong, C., Siribhakdi, K.,
1037 Chuaviroj, S., and Charoenravat, A., 1997. Tertiary diachronic extrusion and
1038 deformation of western Indochina: Structural and $^{40}Ar/^{39}Ar$ evidence from NW
1039 Thailand. Journal of Geophysical Research 102, 10,013-10,037.
1040 Lee, T-Y., and Lawver, L.A., 1995. Cenozoic Plate reconstruction of Southeast Asia.
1041 Tectonophysics 251, 85-138.

1042 Leloup, P.H., Arnaud, N., Lacassin, R., Kienast, J.R., Harrison, T.M., Phan Trong, T.T.,
1043 Replumaz, A., and Tapponnier, P., 2001. New constraints on the structure,
1044 thermochronology, and timing of the Ailao Shan-Red River shear zone, SE Asia.
1045 Journal of Geophysical Research 106, 6683-6732.
1046 Leloup, P.H., Lacassin, R., Tapponnier, P., Schärer, U., Dalai, Z., Xiaohan, L.,
1047 Liangshang, Z., Shaocheng, J., and Trinh, P.T., 1995. The Aliao Shan-Red River
1048 shear zone (Yunnan, China), Tertiary transform boundary of Indochina.
1049 Tectonophysics 251, 3-84.
1050 Lepvrier, C., Maluski, H., Van Tich, V., Leyroloup, A., Thi, P.T., and Vuong, N.V.,
1051 2004. The Early Triassic Indosinian orogeny in Vietnam (Truong Son Belt and
1052 Kontum Massif); implications for the geodynamic evolution of Indochina.
1053 Tectonophysics 393, 87-118.
1054 Maung, H., 1987. Transcurrent movements in the Burma – Andaman sea region. Geology
1055 15, 911-912.
1056 McCourt, W.J., Crow, M.J., Cobbing, E.J., and Amin, T.C., 1996. Mesozoic and
1057 Cenozoic plutonic evolution of SE Asia: evidence from Sumatra, Indonesia. In:
1058 Hall, R., and Blundell, D., (Eds), Tectonic Evolution of Southeast Asia,
1059 Geological Society Special Publication 106, 321-335.
1060 Metcalfe, I., 1991. Late Palaeozoic and Mesozoic palaeogeography of Southeast Asia.
1061 Palaeogeography, Palaeoclimatology, Palaeoecology 87, 211-221.
1062 Metcalfe, I., 1996. Pre – Cretaceous evolution of SE Asian terranes. In: Hall, R., and
1063 Blundell, D., (Eds), Tectonic Evolution of Southeast Asia, Geological Society
1064 Special Publication 106, 97-122.

1065 Metcalfe, I., 2002. Permian tectonic framework and palaeogeography of SE Asia. Journal
1066 of Asian Earth Sciences 20, 551-566.
1067 Metcalfe, I., 2006. Palaeozoic and Mesozoic tectonic evolution and palaeogeography of
1068 East Asian crustal fragments: The Korean Peninsula in context. Gondwana
1069 Research 9, 24-46.
1070 Mitchell, A.H.G., 1981. Phanerozoic plate boundaries in mainland SE Asia, the
1071 Himalayas and Tibet. Journal of the Geological Society of London 138, 109-122.
1072 Mitchell, A.H.G., 1993. Cretaceous – Cenozoic tectonic events in the western Myanmar
1073 (Burma) – Assam region. Journal of the Geological Society, London 150, 1089-
1074 1102.
1075 Mitchell, A.H.G., Htay, M.T., Htun, K.M., Win, M.N., Oo, T., and Hlaing, T., 2007.
1076 Rock relationships in the Mogok metamorphic belt, Tatkon to Mandalay, central
1077 Myanmar. Journal of Asian Earth Sciences 29, 891-910.
1078 Molnar, P., and Tapponnier, P., 1975. Cenozoic tectonics of Asia: effects of a continental
1079 collision. Science 189, 419-426.
1080 Morley, C.K., 2001. Combined escape tectonics and subduction rollback-back arc
1081 extension: a model for the evolution of Tertiary rift basins in Thailand, Malaysia
1082 and Laos. Journal of the Geological Society, London 158, 461-474.
1083 Morley, C.K., 2002. A tectonic model for the Tertiary evolution of strike-slip faults and
1084 rift basins in SE Asia. Tectonophysics 347, 189-215.
1085
1086 Morley, C.K., 2004. Nested strike-slip duplexes, and other evidence for Late Cretaceous-
1087 Palaeogene transpressional tectonics before and during India-Eurasia collision, in

Thailand, Myanmar and Malaysia. Journal of the Geological Society, London 161, 799-812.

Morley, C.K., and Westaway, R., 2006. Subsidence in the super-deep Pattani and Malay basins of Southeast Asia: a coupled model incorporating lower-crustal flow in response to post-rift sediment loading. Basin Research 18, 51-84.

Morley, C.K., Smith, M., Carter, A., Charusiri, P., and Chantraprasert, S., 2007. Evolution of deformation styles at a major restraining bend, constraints from cooling histories, Mae Ping fault zone, western Thailand. In: Cunningham, W.D., and Mann, P., (eds), Tectonics of Strike-Slip Restraining and Releasing Bends, Geological Society, London, Special Publications 290, 325-349.

Moyen, J.-F., Nédélec, A., Martin, H., Jayananda, M., 2003. Syntectonic granite emplacement at different structural levels: the Closepet granite, South India. Journal of Structural Geology 25, 611-631.

Nakapadungrat, S., Jungyusuk, N., Putthapiban, P., Kosuwan, S., and Chaimanee, N., 1991. Southern Thailand: Lithophile mineral deposits (Ranong – Takua Pa – Phuket). The Seventh Regional Conference on Geology, Mineral and Energy Resources of Southeast Asia and The Third Symposium IGCP 282: Rare Metal Granitoids. Geological excursion guidebook no.2, 76 pp.

Packham, G.H., 1993. Plate tectonics and the development of sedimentary basins of the dextral regime in western Southeast Asia. Journal of Southeast Asian Earth Sciences 8, 497-511.

Passchier, C.W., and Simpson, C., 1986. Porphyroclast systems as kinematic indicators. Journal of Structural Geology 8, 831-843.

1111 Passchier, C.W., and Trouw, R.A.J., 2005. Microtectonics, 2nd Edition. Springer-Verlag,
1112 Germany, 366pp.
1113 Pigott, J.D., and Sattayarak, N., 1993. Aspects of sedimentary basin evolution assessed
1114 through tectonic subsidence analysis. Example: northern Gulf of Thailand.
1115 Journal of Southeast Asian Earth Sciences 8, 407-420.
1116 Pivnik, D.A., Nahm, J., Tucker, R.S., Smith, G.O., Nyein, K., Nyunt, M., Maung, P.H.,
1117 1998. Polyphase deformation in a fore-arc/back-arc basin, Salin subbasin,
1118 Myanmar (Burma), American Association of Petroleum Geologists Bulletin 82,
1119 1837-1856.
1120 Polachan, S., 1988. The Geological Evolution of the Mergui Basin, S.E. Andaman Sea,
1121 Thailand. Unpublished PhD Thesis, Royal Holloway and Bedford New College,
1122 University of London, 218 pp.
1123 Polachan, S., Pradidtan, S., Tongtaow, C., Janmaha, S., Intarawijitr, K., and Sangsuwan,
1124 C., 1991. Development of Cenozoic basins in Thailand. Marine and Petroleum
1125 Geology 8, 84-97.
1126 Putthapiban, P., 1992. The Cretaceous – Tertiary granite magmatism in the west coast of
1127 peninsular Thailand and the Mergui Archipelago of Myanmar/Burma. National
1128 Conference on "Geological Resources of Thailand: Potential for Future
1129 Development", Department of Mineral resources, Bangkok, Thailand, 75-88.
1130 Putthapiban, P., and Schwartz, M.O., 1994. Geochronology of the Southeast Asian tin
1131 belt granitoids. In: Seltmann, Kämpf and Möller (eds), Metallogeny of Collisional
1132 Orogens, Czech Geological Survey, Prague, 391-398.

1133 Ramana, M.V., Nair, R.R., Sarma, K.V.L.N.S., Ramprasad, T., Krishna, K.S.,
1134 Subrahmanyam, V., D'Cruz, M., Subrahmanyam, C., Paul, J., Subrahmanyam,
1135 A.S., and Chandra Sekhar, D.V., 1994. Mesozoic anomalies in the Bay of Bengal.
1136 Earth and Planetary Science Letters 121, 469-475.
1137 Rangin, C., Klein, M., Roques, D., Le Pichon, X, and Van Trong, L., 1995. The Red
1138 River fault system in the Tonkin Gulf, Vietnam. Tectonophysics 243, 209-222.
1139 Replumaz, A., and Tapponnier, P., 2003. Reconstruction of the deformed collision zone
1140 between India and Asia by backward motion of lithospheric blocks. Journal of
1141 Geophysical Research 108, ETG 1-1 – 1-24.
1142 Ridd, M.F., 1978. Thailand. In: Moulladem, M., and Nairn, A.E.M., (eds.), The
1143 Phanerozoic Geology of the World, II, The Mesozoic, A., Elsevier, Amsterdam,
1144 145-163.
1145 Royer, J.Y., and Sandwell, D.T., 1989. Evolution of the Eastern Indian Ocean since the
1146 Late Cretaceous; constraints from Geosat Altimetry. Journal of Geophysical
1147 Research 94B, 13755-13782.
1148 Schwartz, M.O., Rajah,S.S., Askury, A.K., Putthapiban, P., and Djaswadi, S., 1995. The
1149 Southeast Asian Tin Belt. Earth-Science Reviews 38, 95-293.
1150 Searle, M., Corfield, R.I., Stephenson, B., and McCarron, J., 1997. Structure of the North
1151 Indian continental margin in the Ladakh-Zanskar Himalayas: implications for the
1152 timing of obduction of the Spontang ophiolite, India-Asia collision and
1153 deformation events in the Himalaya. Geological Magazine 134, 297-316.

1154 Searle, M.P., 2006. Role of the Red River Shear zone, Yunnan and Vietnam, in the
1155 continental extrusion of SE Asia. Journal of the Geological Society, London 163,
1156 1025-1036.
1157 Searle, M.P., Noble, S.R., Cottle, D.J., Waters, D.J., Mitchell, A.H.G., Hlaing, T., and
1158 Horstwood, M.S.A., 2007. Tectonic evolution of the Mogok metamorphic belt,
1159 Burma (Myanmar) constrained by U-Th-Pb dating of metamorphic and magmatic
1160 rocks. Tectonics 26, TC3014.
1161 Smyth, H., 2005. Eocene to Miocene basin history and volcanic activity in East Java,
1162 Indonesia. Unpublished PhD Thesis, Royal Holloway, University of London, 476
1163 pp.
1164 Smyth, H., Hamilton, P.J., Hall, R., and Kinny, P.D., 2007. The deep crust beneath island
1165 arcs: Inherited zircons reveal a Gondwana continental fragment beneath East
1166 Java, Indonesia. Earth and Planetary Science Letters 258, 269-282.
1167 Stipp, M., Stünitz, H., Heilbronner, R., and Schmid, S.M., 2002. The eastern Tonale fault
1168 zone: a 'natural laboratory' for crystal plastic deformation of quartz over a
1169 temperature range from 250 to 700 °C. Journal of Structural Geology 24, 1861-
1170 1884.
1171 Tapponnier, P., Peltzer, G., and Armijo, R., 1986. On the mechanics of the collision
1172 between India and Asia. In: Coward, M.P., and Ries, A.C., (eds), Collision
1173 Tectonics, Geological Society Special Publication 19, 115-157.
1174 Tapponnier, P., Peltzer, G., Le Dain, A.Y., Armijo, R., and Cobbold, P., 1982.
1175 Propagating extrusion tectonics in Asia: New insights from simple experiments
1176 with plasticine. Geology 10, 611-616.

1177 Upton, D.R., 1999. A regional fission track study of Thailand: implications for thermal
1178 history and denudation. Unpublished PhD Thesis, Royal Holloway University of
1179 London, UK, 392 pp.
1180 van der Voo, R., Spakman, W., and Bijwaard, H., 1999. Tethyan subducted slabs under
1181 India. Earth and Planetary Science Letters 171, 7-20.
1182 Wang, E., Burchfiel, B.C., Royden, L.H., Liangzhong, C., Jishen, C., Wenxin, L., and
1183 Zhiliang, C., 1998. Late Cenozoic Xianshuihe-Xiaojiang, Red River, and Dali
1184 fault systems of Southwestern Sichuan and Central Yunnan, China. Boulder,
1185 Colorado, Geological Society of America Special Paper 327, 108pp.
1186 Zaw, K., 1990. Geological, petrological and geochemical characteristics of granitoid
1187 rocks in Burma: with special reference to the associated W–Sn mineralisation and
1188 their tectonic setting. Journal of Southeast Asian Earth Sciences 4, 293–335.
1189
1190

1191 ## Figure captions

1192 **Fig. 1.** Regional tectonic elements of mainland Southeast Asia. Horizontal line ornament:
1193 Western Province granites; dotted ornament: Main Range granites; vertical line
1194 ornament: Eastern Province granites; pale grey: Tertiary basins; black lines: brittle faults;
1195 grey half arrows: ductile shear sense; black half arrows: brittle shear sense. After
1196 Cobbing et al. (1986); Morley (2002); Polachan (1988).

1197

1198 **Fig. 2.** Detail of the Thai Peninsula showing the Ranong and Khlong Marui fault zones.
1199 (a.) Fault map. Ornament as before, except dark grey: metamorphic cores. Granite
1200 outlines modified from Department of Mineral Resources (1982), and basin outlines from
1201 Intawong (2006). (b.) SRTM (Shuttle Radar Topography Mission) digital elevation
1202 model of the same area.

1203

1204 **Fig. 3.** Field photographs from the KMF and RF, all except (b.) looking onto sub-
1205 horizontal surfaces. (a.) Weakly stretched pebble in metasediments sheared during D_1.
1206 Faint pressure shadows indicate dextral shear sense. (b.) Road cut section near La-Un on
1207 the RF showing large scale kink band in S_1, formed at the end of D_1. (c.) Outcrop of
1208 characteristic stromatic migmatite from the high melt volume migmatites of the RF, at the
1209 Myanmar border NW of Tha Sae. Pen is 159 mm long. (d.) S-C' fabric developed in a
1210 greenschist facies granite mylonite near Ban Set Takuat, Ranong. (e.) Typical ellipsoidal
1211 boudins of leucosome in a river polished section of low melt migmatites from the isolated
1212 ductile core north of Kapoe, in the RF. (f.) River polished section showing disharmonic,

1213 rootless folding of a thin leucosome band in the low melt migmatites from the eastern
1214 side of the KMF ductile core.
1215
1216 **Fig. 4.** Map of the RF ductile core which truncates the pre-D_2 Ranong Granite at Ranong.
1217 Granite and sedimentary geology modified after Department of Mineral Resources (1982,
1218 1992). Bold asterisks indicate tie points used to calculate sinistral displacement. See
1219 sections 3.3 and 4.1 for details. D_1 and D_2 equal area southern hemisphere stereonets
1220 show poles to ductile foliation (open circles) and ductile lineations (filled circles). D_3 and
1221 D_4 stereonets show poles to fault planes (open circles) and slickenside lineations (filled
1222 circles). Section A-A' shows a representative section through the core. Folding is
1223 schematic and illustrates style and intensity. Dashed lines: foliation in metamorphic
1224 rocks, bedding in sedimentary rocks; bold lines: main strike-slip faults. All kinematic
1225 indicators refer to D_3 faults. For location see Fig. 2.
1226
1227 **Fig. 5.** Map of the RF ductile core north of Ban Pak Chan. Details as for Fig. 4, except
1228 sedimentary geology modified after Department of Mineral Resources (2006).
1229
1230 **Fig. 6.** Map of the RF ductile cores west of Bang Saphan Noi. Details as for Fig. 4.
1231
1232 **Fig. 7.** Map of the KMF ductile core: Khao Phanom, north-east of Phang Nga. Details as
1233 for Fig. 4.
1234

Fig. 8. Field photographs of brittle structures in the KMF and RF. All except (a.) and (c.) looking onto sub-horizontal surfaces. (a.) Limestone mountains north of Thap Put, marking the trace of a steeply dipping D_3 minor strand of the KMF. (b.) Polished section of weakly foliated fault breccia from a D_3 brittle strand within the KMF ductile core at Khao Phanom. Clasts are mostly fragments of D_2 mylonite, found in nearby intact units. (c.) Fault plane showing an older sinistral strike-slip fault with a small reverse oblique component, reactivated in a normal sense. Exposed within a 2 m wide zone of cataclasis near the northwestern edge of the KMF. (d.) Minor sinistral fault (marked by dashed line) associated with D_3 on the RF west of Bang Saphan Noi. Pale offset surface is a migmatite leucosome. Pen for scale below fault plane. (e.) En-echelon Riedel fault array formed during D_4 showing a slight dextral offset of the banded mylonites through which it cuts. RF, north of Ban Pak Chan. (f.) Quartz segregation in KMF quartz-biotite mylonites, showing a dextral offset along a typically oblique D_4 fault.

Fig. 9. Transect through the ductile core at Khao Plai Khlong Hin Phao north of Ban Pak Chan. $D_1 – D_2$ foliation shown by dip and strike symbols. Bold lines indicate major D_3 faults. Small fault maps illustrate typical D_4 structures developed in all lithologies. Pale grey bands represent deformed foliation parallel ductile markers such as stromatic leucosomes and stretched objects. D_4 fault scale bars are 10 cm long. Whole map and D_4 figures rotated 20° anticlockwise.

Fig. 10. Regional reconstruction in Late Cretaceous times. Based on Charusiri et al. (1993); Hall (2002); Mitchell (1993); Mitchell et al. (2007); Morley (2002); Searle et al.

(2007). After restoration of Neogene movements on the Sagaing Fault and Andaman Sea, Western Burma lies outboard of Northern Thailand, close to the KMF and RF. The change from an inactive trench offshore Sumatra to active subduction offshore Western Burma is adjacent to the position of the KMF.

Fig. 11. Schematic block diagram illustrating major processes during deformation of the KMF and RF. Metamorphic fault rocks of one or more ductile shear zones, indicated by grey shading, cut and are cut by granitoid intrusions, and contain foliation parallel syn-kinematic intrusions at deeper levels. Post kinematic granites are widespread, and are emplaced outside the main fault zone. Transpressive sinistral faulting during D_3 forces slivers of the older shear zone to the surface in positive flower structures, which cross cut all older features. These brittle faults may be rooted in ductile shear zones at depth. Grey kinematic indicators represent $D_1 - D_2$, black represents D_3.

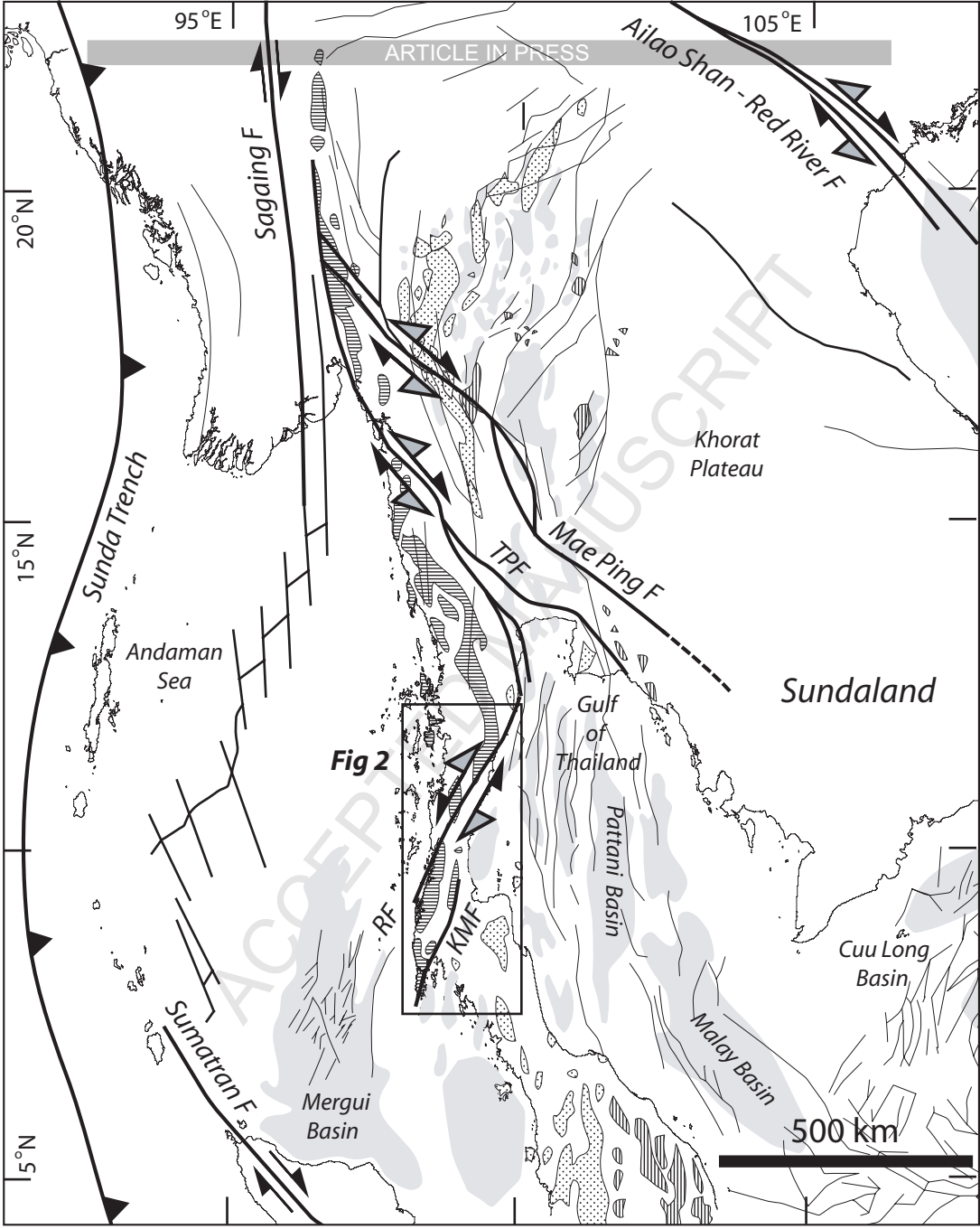

Figure 1

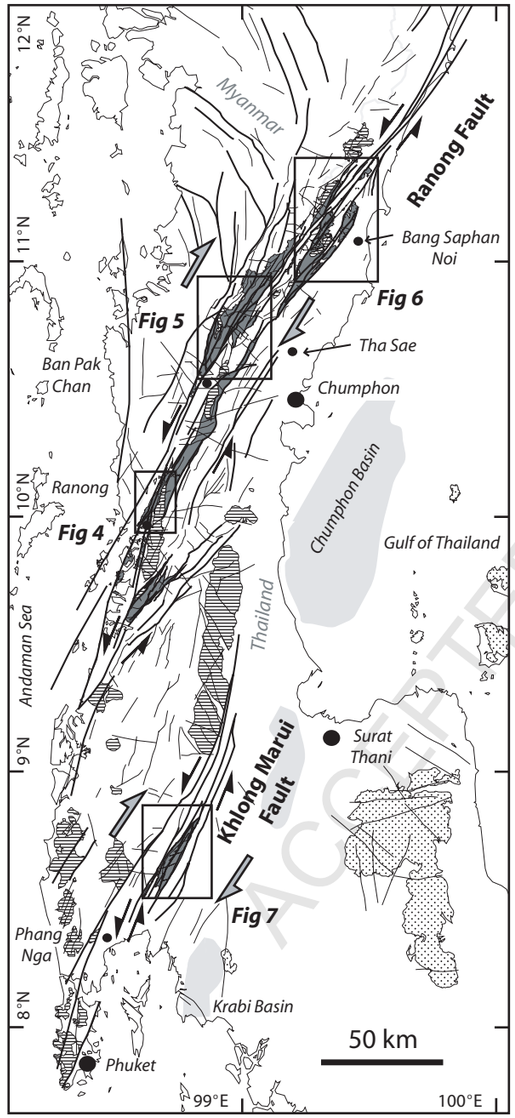

a.)

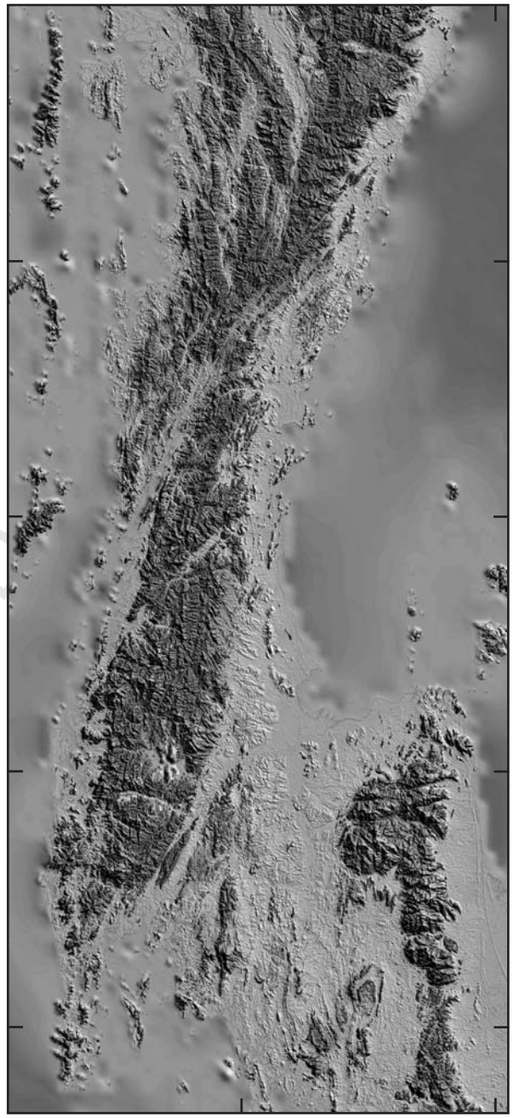

b.)

Figure 2

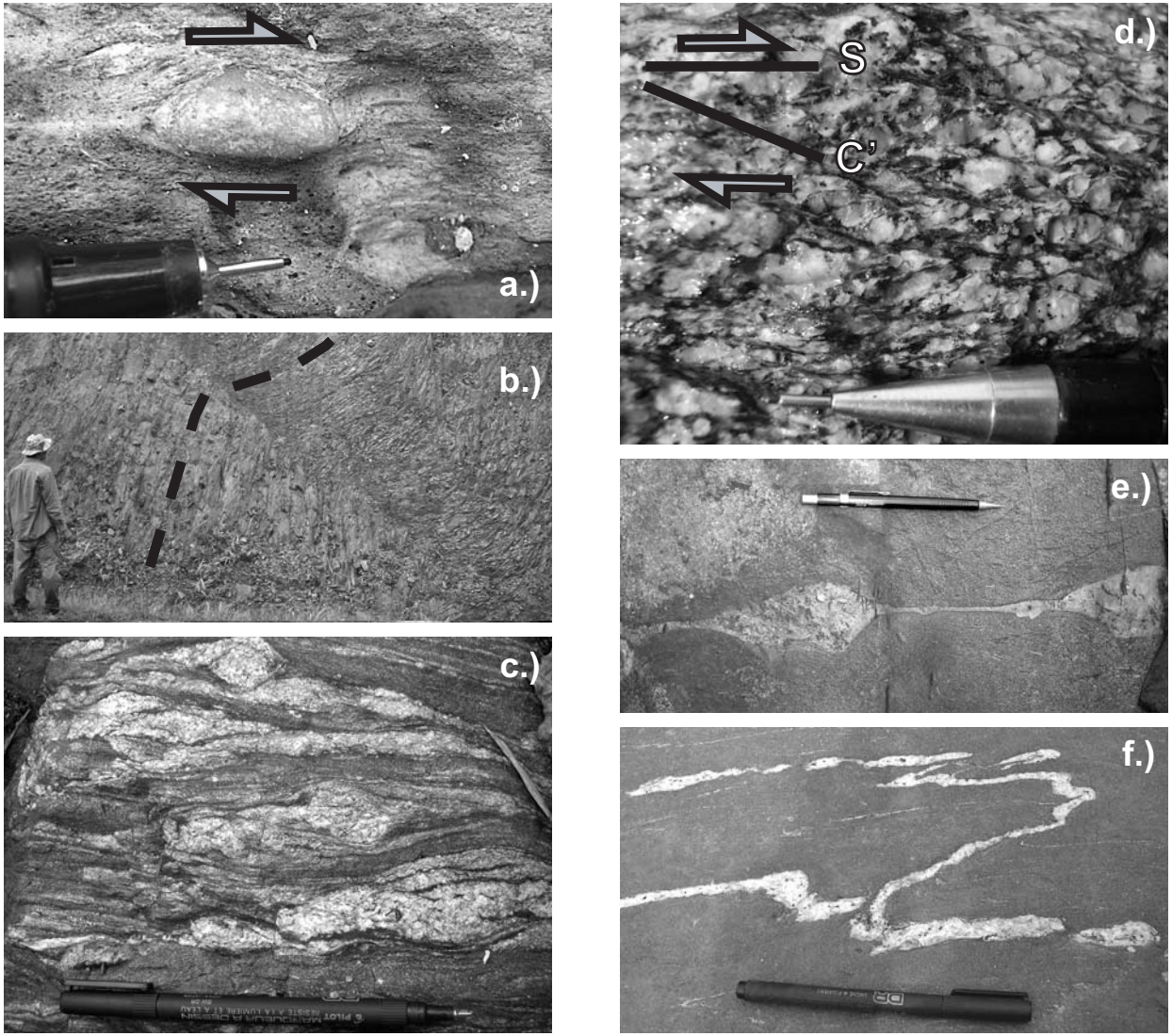

Figure 3

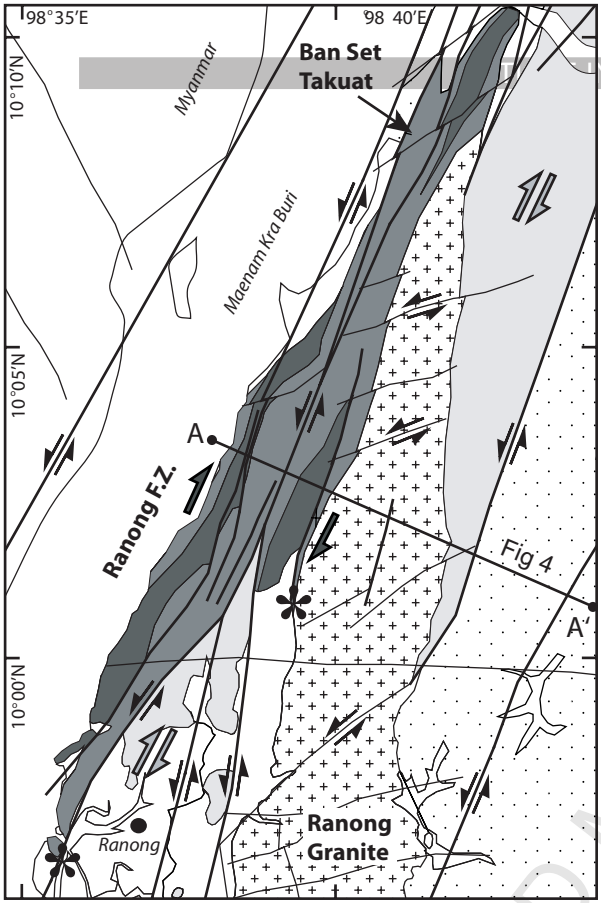

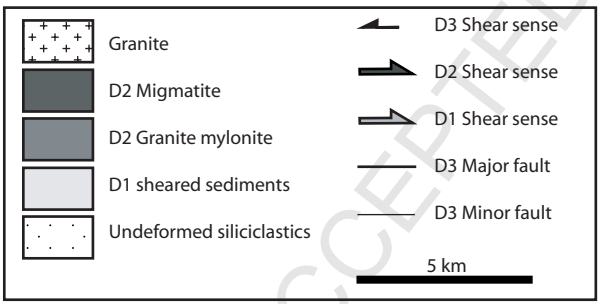

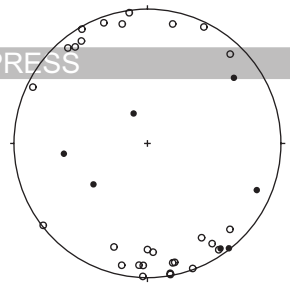

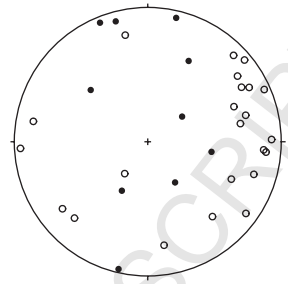

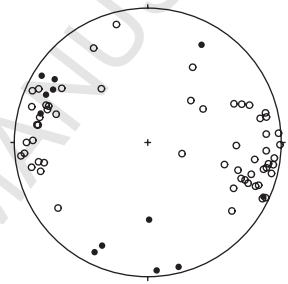

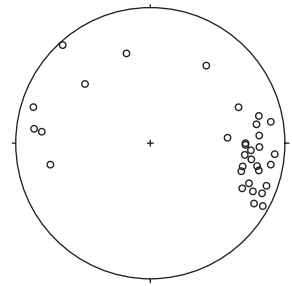

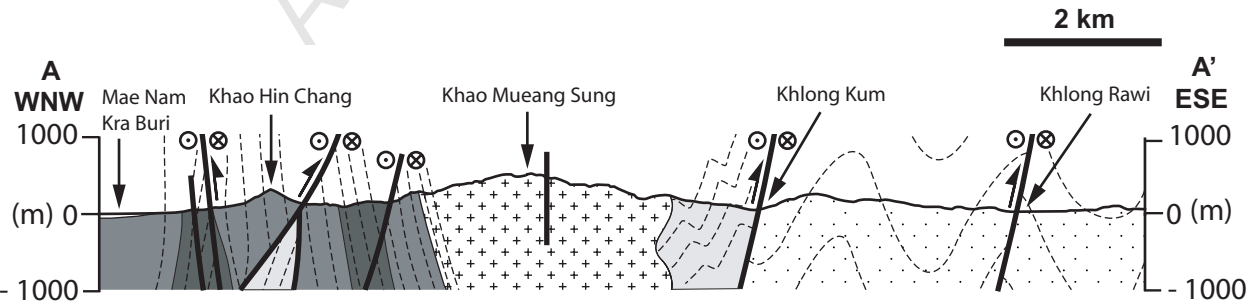

Figure 4

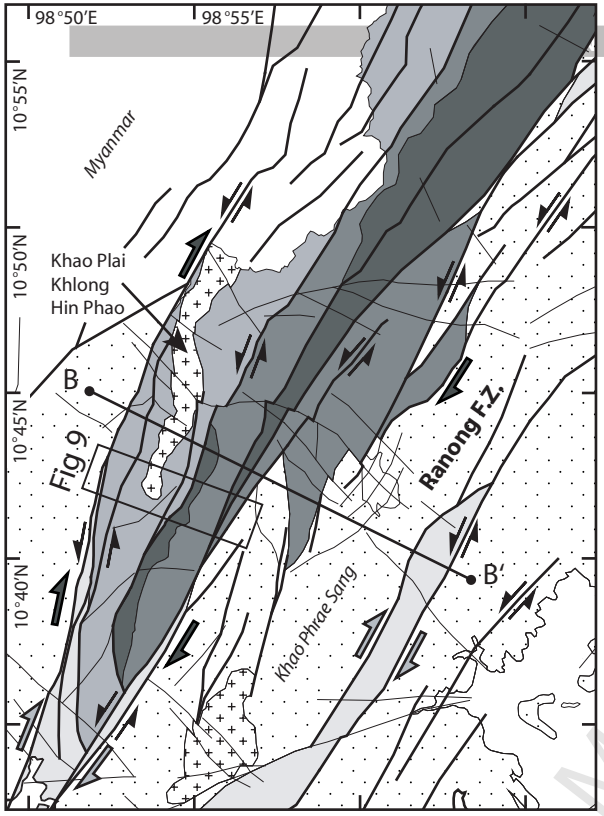

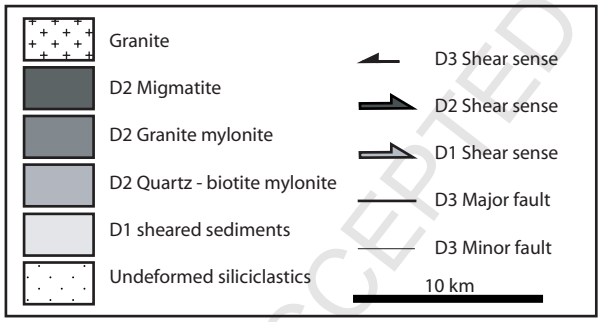

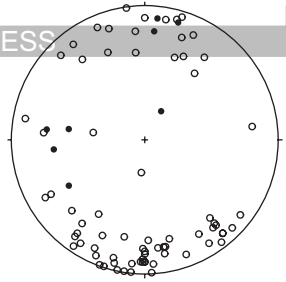

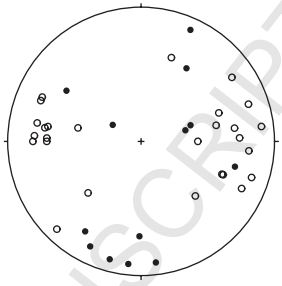

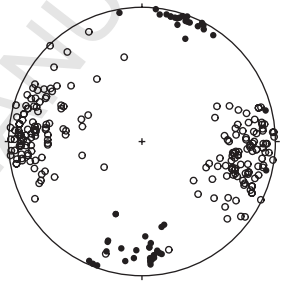

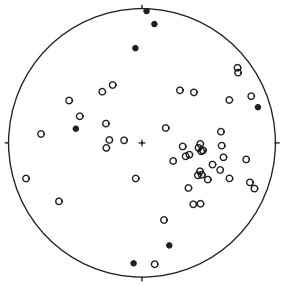

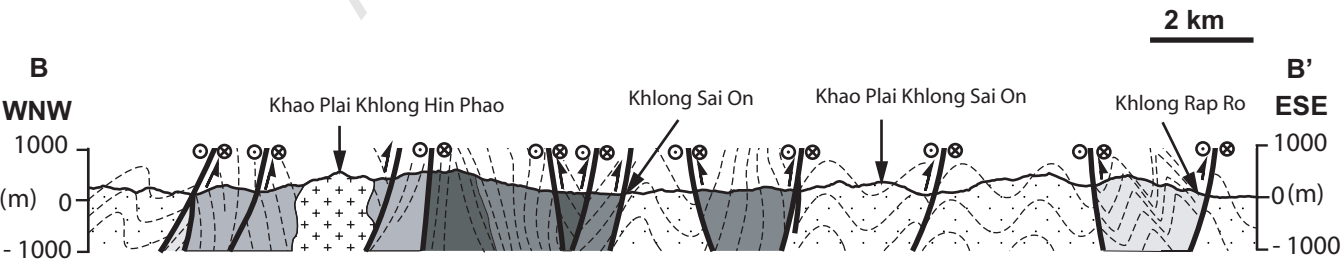

Figure 5

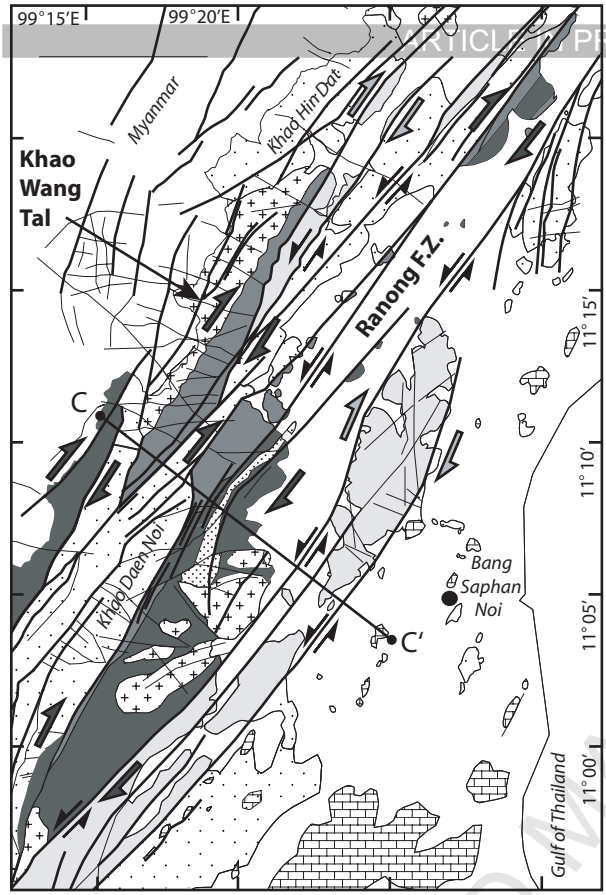

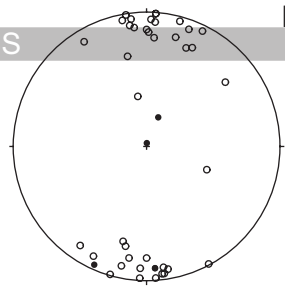

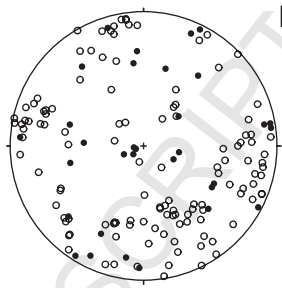

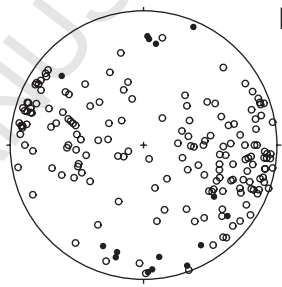

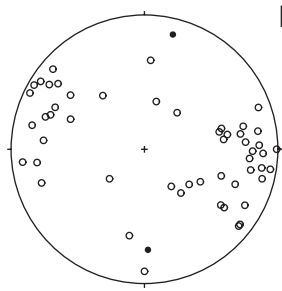

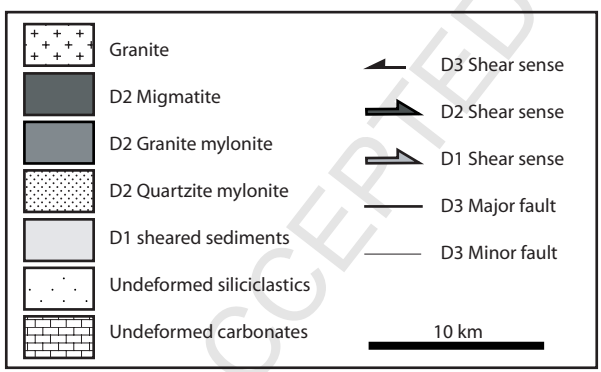

2 km

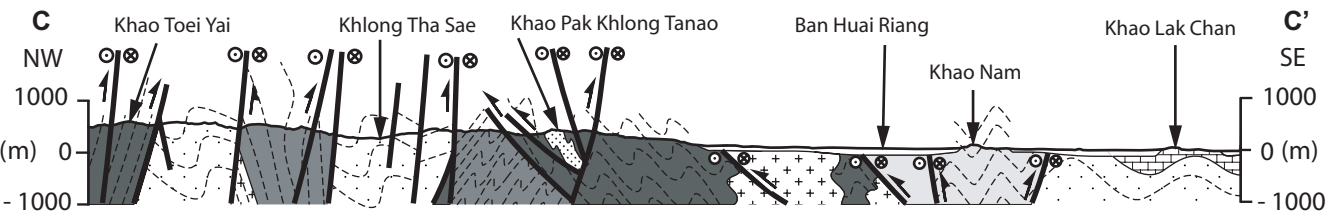

Figure 6

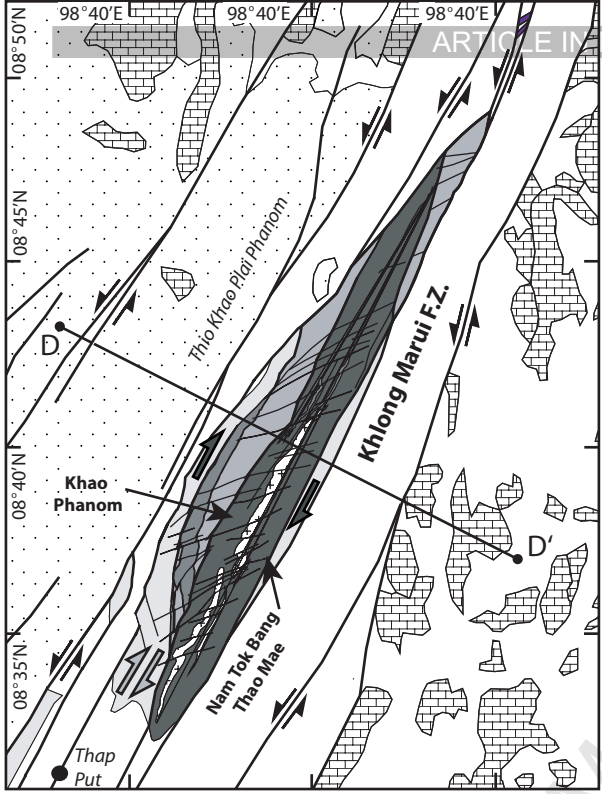

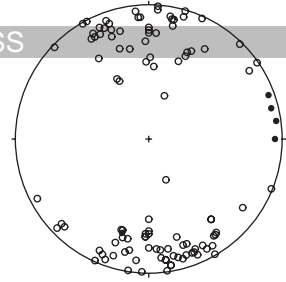

D4 Faults and slickensides

○ 106
● 5

D3 Faults and slickensides

○ 193
● 91

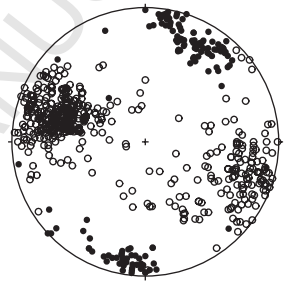

D2 Foliations and lineations

○ 470
● 142

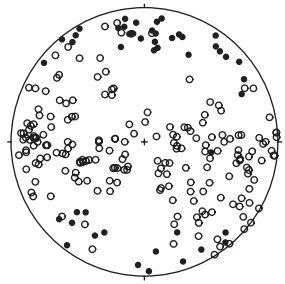

D1 Foliations and lineations

○ 197
● 47

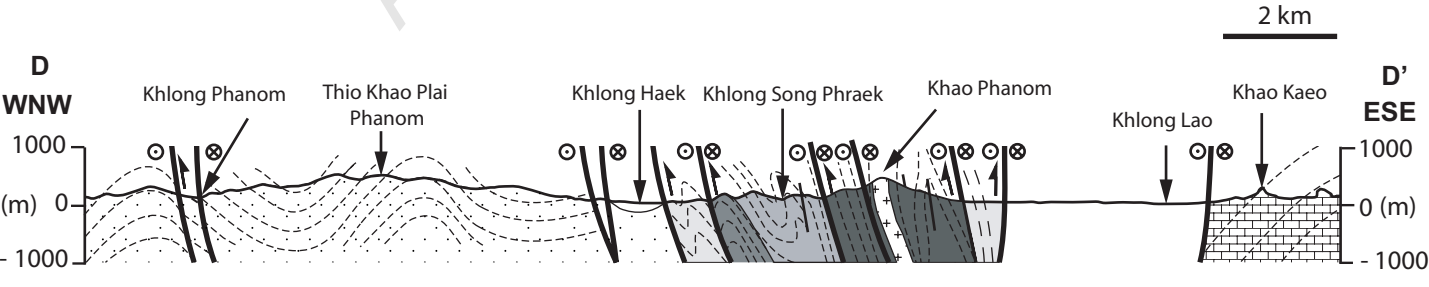

Figure 7

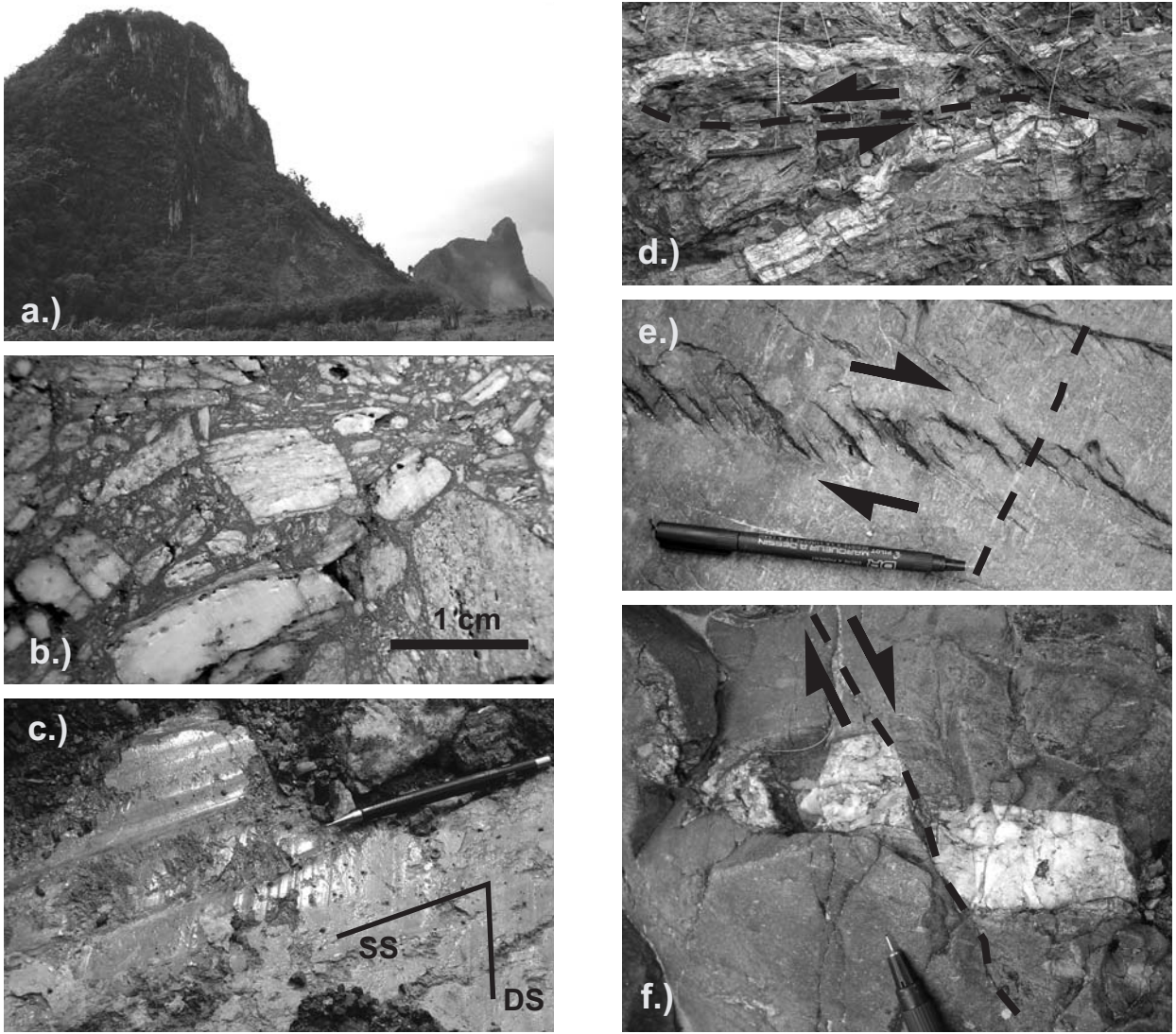

Figure 8

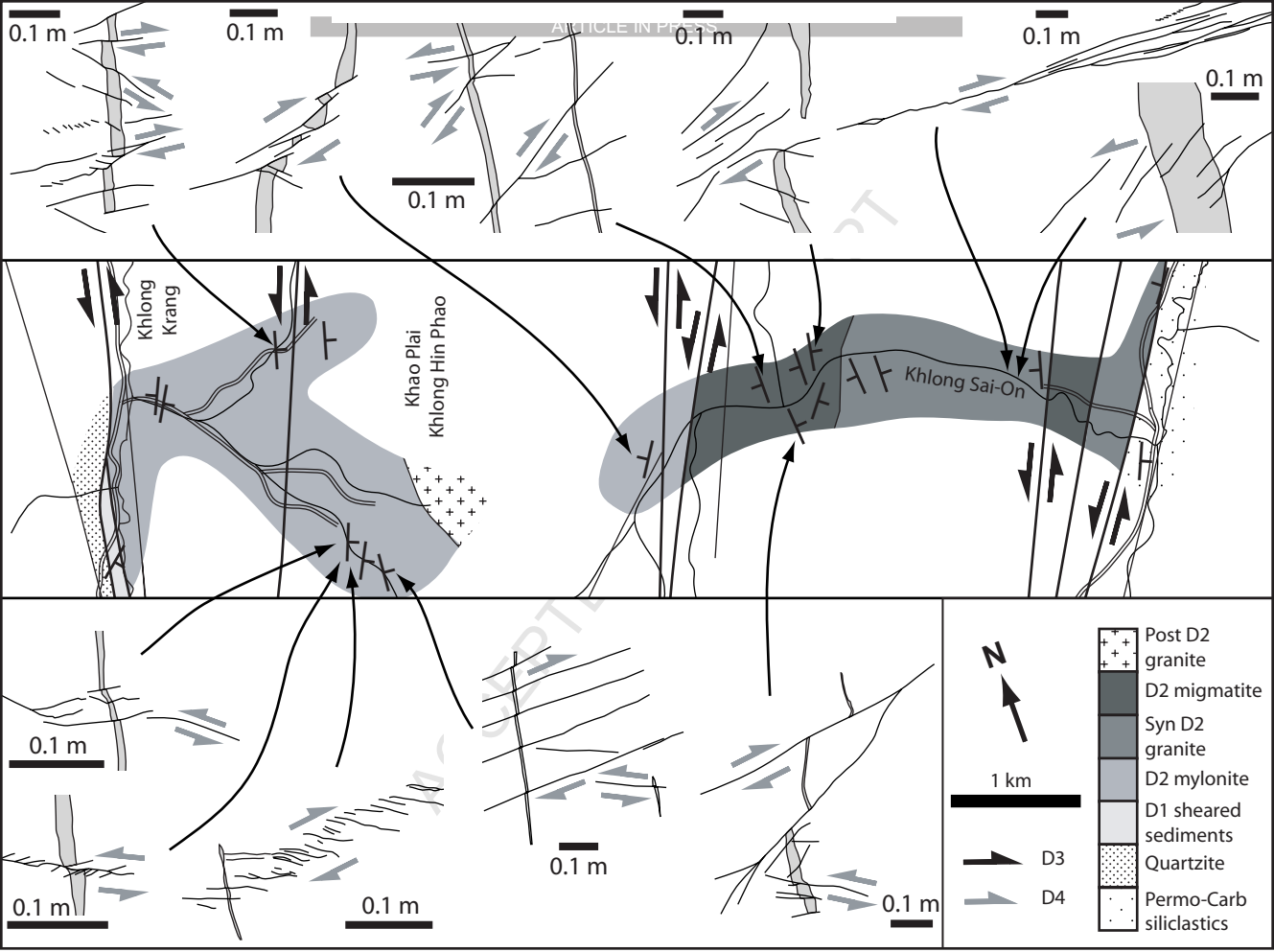
0.1 m
0.1 m
0.1 m
0.1 m
0.1 m
Khlong Krang
Khao Plai Khlong Hin Phao
Khlong Sai-On
0.1 m
0.1 m
0.1 m
0.1 m
N
1 km
D3
D4
Post D2 granite
D2 migmatite
Syn D2 granite
D2 mylonite
D1 sheared sediments
Quartzite
Permo-Carb siliclastics

Figure 9

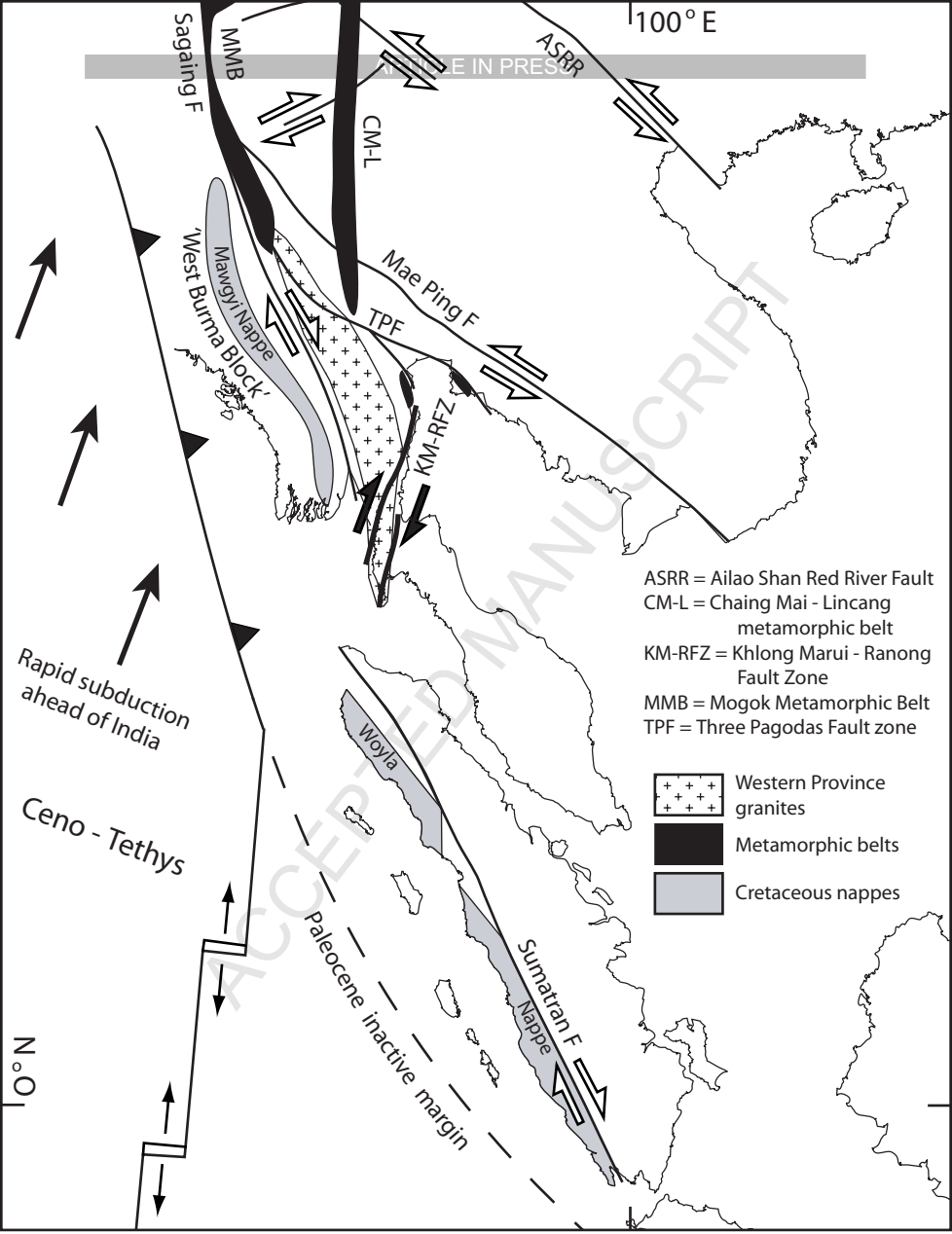

Figure 10

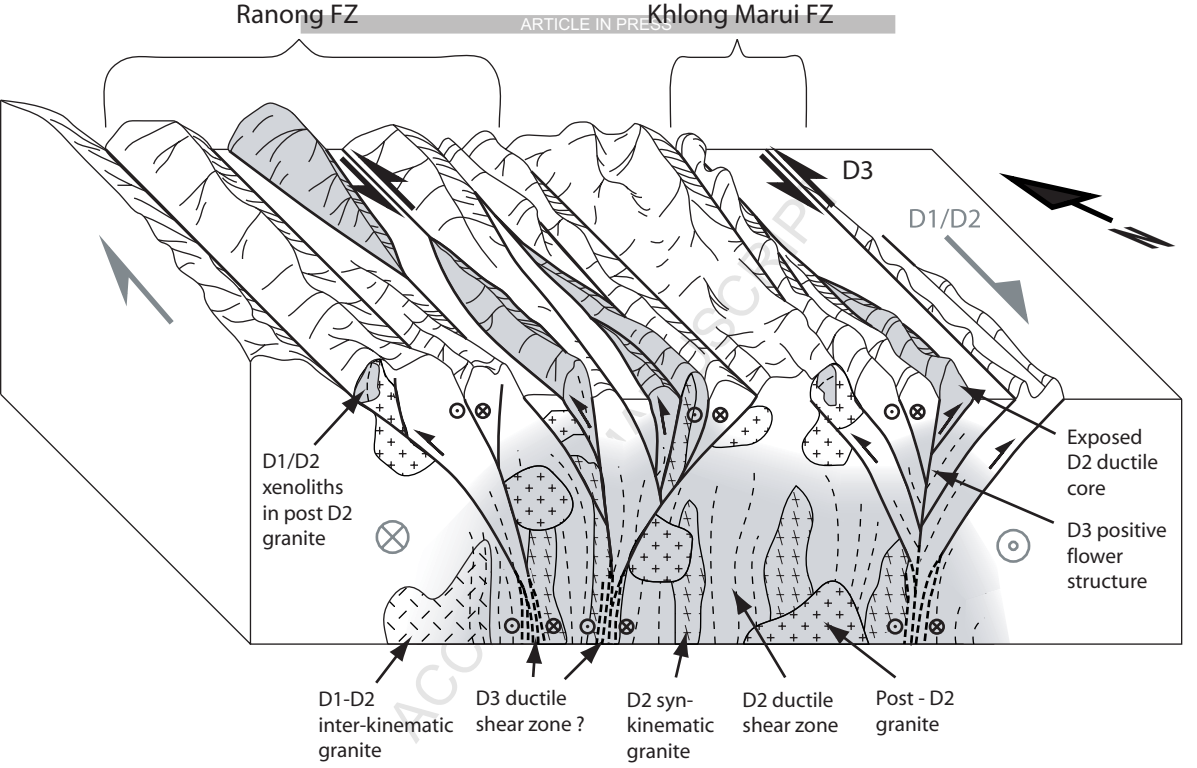

Figure 11